

A SPECIFIC INORGANIC TRIPHOSPHATASE FROM *NITROSOMONAS EUROPAEA*:
STRUCTURE AND CATALYTIC MECHANISM*

David Delvaux^{‡1}, Mamidanna R.V.S. Murty^{§1|2}, Valérie Gabelica^{§3}, Bernard Lakaye^{‡3}, Vladimir V. Lunin^{¶4}, Tatiana Skarina[¶], Olena Onopriyenko[¶], Gregory Kohn[‡], Pierre Wins[‡], Edwin De Pauw[§] and Lucien Bettendorff^{‡5}

From the [‡]GIGA-Neuroscience and the [§]GIGA Systems Biology and Chemical Biology, University of Liège, B-4000 Liège, Belgium
and the [¶]Banting and Best Department of Medical Research, University of Toronto, Toronto, Ontario, M5G 1L6, Canada

Running head: A specific inorganic triphosphatase from *Nitrosomonas europaea*

Address correspondence to L. Bettendorff, Unit of Bioenergetics and cerebral excitability, GIGA-Neurosciences, University of Liège, avenue de l'Hôpital, 1, 4000 Liège, Belgium. Tel.: +32 4 366 59 67, Fax: + 32 4 366 59 53, Email: L.Bettendorff@ulg.ac.be

The CYTH superfamily of proteins is named after its two founding members, the CyaB adenylyl cyclase from *Aeromonas hydrophila* and the human 25-kDa thiamine triphosphatase. Because these proteins often form a closed β -barrel, they are also referred to as “Triphosphate Tunnel Metalloenzymes” (TTM). Functionally, they are characterized by their ability to bind triphosphorylated substrates and divalent metal ions. These proteins exist in most organisms and catalyze different reactions, depending on their origin. Here we investigate structural and catalytic properties of the recombinant TTM protein from *Nitrosomonas europaea* (*NeuTTM*), a 19-kDa protein. Crystallographic data show that it crystallizes as a dimer and that, in contrast to other TTM proteins, it has an open β -barrel structure. We demonstrate that *NeuTTM* is a highly specific inorganic triphosphatase, hydrolyzing tripolyphosphate (PPP_i) with high catalytic efficiency in the presence of Mg²⁺. These data are supported by native mass spectrometry analysis showing that the enzyme binds PPP_i (and Mg-PPP_i) with high affinity ($K_d < 1.5 \mu\text{M}$), while it has a low affinity for ATP or thiamine triphosphate. In contrast to *Aeromonas* and *Yersinia* CyaB proteins, *NeuTTM* has no adenylyl cyclase activity, but it shares several properties with other enzymes of the CYTH superfamily, e.g. heat-stability, alkaline pH optimum and inhibition by Ca²⁺ and Zn²⁺ ions. We suggest a catalytic mechanism involving a catalytic dyad formed by K52 and Y28. The present data provide the first characterization of a new type of phosphohydrolase (unrelated to pyrophos-

phatases or exopolyphosphatases), able to hydrolyze inorganic triphosphate with high specificity.

A large number of phosphohydrolases are able to hydrolyze triphosphorylated compounds, generally nucleoside triphosphates such as ATP or GTP. However, in 2002, we achieved the molecular characterization of a mammalian enzyme that specifically hydrolyzed thiamine triphosphate (ThTP⁶), a compound unrelated to nucleotides (1). This 25-kDa soluble thiamine triphosphatase (ThTPase), which is involved in the regulation of cytosolic ThTP concentrations (2), has near absolute specificity for ThTP (it does not hydrolyze nucleotides) and a high catalytic efficiency. No sequence homology with other known mammalian proteins could be found.

Shortly thereafter, Iyer and Aravind (3) observed that the catalytic domains of human 25-kDa ThTPase (1) and CyaB adenylyl cyclase (AC2) from *Aeromonas hydrophila* (4) define a novel superfamily of domains that, according to these authors, should bind “organic phosphates”. This superfamily was called “CYTH” (CYaB-THiamine triphosphatase), and the presence of orthologs was demonstrated in all three superkingdoms of life. This suggested that CYTH is an ancient family of proteins, and that a representative must have been present in the last universal common ancestor (LUCA) of all extant life forms. It was proposed (3) that this enzymatic domain might play a central role at the interface between nucleotide and polyphosphate metabolism, but this role remains largely undefined: in fact, the two structurally

and enzymatically characterized members of the superfamily, AC2 and mammalian 25-kDa ThTPase, are likely to be secondary acquired activities, while other prokaryotic CYTH proteins would have performed more ancient and fundamental roles in organic phosphate and/or polyphosphate metabolism (3).

Using multiple alignments and secondary structure predictions, Iyer and Aravind showed that the catalytic core of CYTH enzymes contained a novel $\alpha + \beta$ scaffold with 6 conserved acidic and 4 basic residues. At least 4 of the acidic residues (generally glutamate) are likely to chelate divalent cations required for catalysis, as is the case for adenylyl cyclases, DNA polymerases and some phosphohydrolases (3,5,6).

More recently and independently of those bioinformatic studies, Shuman and coworkers pointed out that RNA triphosphatases of fungi and protozoa exhibit striking similarities with bacterial and archaeal proteins of unknown function that belong to the CYTH superfamily (7). Although the primary structure conservation is low, the active site folds of the Cet1 RNA triphosphatase from *S. cerevisiae* (8) and of several prokaryotic CYTH proteins are remarkably similar: in both cases, an eight-strand antiparallel β -barrel forms a topologically closed tunnel, and triphosphorylated substrates, as well as divalent cation activators, bind in the hydrophilic cavity. Therefore, Shuman and coworkers called these proteins “Triphosphate Tunnel Metalloenzymes” (TTM). They assumed that TTM was a larger superfamily including Cet1-like and CYTH proteins (7).

However, it is not established that all members of the CYTH superfamily exhibit the closed tunnel conformation. For instance, the 25-kDa mouse ThTPase has an open cleft structure when free in solution, while the enzyme-ThTP complex has a more closed, tunnel-like conformation (9). This suggests that the CYTH domain may be a versatile fold, both structurally and functionally.

Despite the presence of orthologs in most organisms, the general significance of CYTH enzymes remains a matter of conjecture. In unicellular eukaryotes, the essential role of RNA triphosphatases in RNA capping is clearly defined. But, like ThTPase activity in mammals, this is probably a secondary adaptation. In bacteria, two CYTH proteins, from *A. hydrophila* (4) and *Yersinia pestis* (10,11) are considered as a particular class of adenylyl

cyclases (“class IV”, CyaB), but this enzyme activity was found to be significant only under rather extreme conditions (50-60 °C and pH around 10). In addition, a more efficient class I adenylyl cyclase is also present in *A. hydrophila* (4) and *Y. pestis* (11). Archaeal and bacterial CYTH proteins have since been annotated as hypothetical (CyaB-like) adenylyl cyclases.

However, a bacterial CYTH ortholog from *Clostridium thermocellum* was recently shown to be completely devoid of adenylyl cyclase activity (12). The enzyme, which was characterized by Shuman and coworkers in considerable detail (12,13) had a rather broad substrate specificity. It hydrolyzed guanosine 5'-tetraphosphate (Gp₄), inorganic triphosphate (tripolyphosphate, PPP_i) and to a lesser extent nucleoside triphosphates and long-chain polyphosphates (12,13).

In 2005, we obtained the three-dimensional crystal structure of the *Nitrosomonas europaea* CYTH ortholog (*NeuTTM*), the hypothetical protein NE1496 (Protein Data Bank 2FBL (14) and, although, labeled as a TTM (12), it rather exhibits a C-shaped cup conformation, or incomplete β -barrel.

Because of the structural similarities between *NeuTTM* and mouse 25-kDa ThTPase (open cleft rather than closed tunnel), we considered the possibility that ThTP might be a good substrate for *NeuTTM*. Indeed, in *E. coli*, ThTP may be involved in responses to environmental stress (15), but no specific bacterial ThTPase has been characterized so far. However, the present data show that *NeuTTM* is actually devoid of significant ThTPase activity (as well as of adenylyl cyclase activity) but that *NeuTTM* has a strong preference and high affinity for PPP_i. Furthermore, we show that two residues that are highly conserved in CYTH proteins (K52 and Y28) are important for catalysis. This is the first characterization of a specific tripolyphosphatase (PPPase), raising the question of the existence and possible role of PPP_i in living cells.

MATERIALS AND METHODS

Materials—Sodium tripolyphosphate (PPP_i), sodium cyclic triphosphate (trimetaphosphate, cPPP_i), polyphosphate (sodium phosphate glass, 65 ± 5 residues), ATP, ITP, GTP and guanosine 5'-tetraphosphate (Gp₄, Tris salt) were from Sigma. Thiamine triphosphate (ThTP) was synthesized and purified as previously described (16). Tetraphosphate (P₄) (initially from Sigma) was a gift from Dr. Eric Oldfield, Department of

Chemistry, University of Illinois, A110 CLSL 600 South Mathews Ave. Urbana, IL 61801. The pET15b vector for the expression of *NeuTTM* as a His-tag fusion protein was a gift from Dr. A. Savchenko, University of Toronto, Banting and Best Department of Medical Research, C.H. Best Institute, Toronto, Ontario, Canada).

Overexpression and purification of NeuTTM—BL21(DE3) *E. coli* cells were transformed with a pET15b plasmid containing the sequence of *NeuTTM* with a 6 His sequence at the N-terminal side of the gene. Transformed bacteria were grown overnight at 37 °C in 2 ml LB medium containing 500 µg/ml ampicillin. Then the bacteria were cultured in 50-200 ml of 2XYT medium containing 250 µg/ml ampicillin until A_{600} reached 0.6-0.8. Expression of the fusion protein was induced with isopropyl β-D-1-thiogalactopyranoside (1 mM). After 3 hours incubation at 37 °C, the bacterial suspension was centrifuged 15 min at 8000 g (4 °C). Bacteria were suspended in modified binding buffer (20 mM HEPES instead of phosphate buffer, 0.5 M NaCl, 30 mM imidazole pH 7.5). After two cycles with a French press disruptor, the lysate was centrifuged 30 min at 50,000 g. The tagged protein was purified on a FPLC system (ÄKTA™ Purifier, Amersham Biosciences) coupled to a 5 ml HisTrap™ FF column (GE Healthcare) in the above-mentioned buffer. *NeuTTM* was then eluted in eluting buffer (20 mM HEPES, 0.5 M NaCl, 0.5 M imidazole, pH adjusted to 7.5 with HCl 6N). Removal of the His-tag was achieved by incubating 1 mg of the purified protein with 200 units of AcTEV™ protease (Invitrogen). After 2 hours at room temperature, the mixture was purified on the HisTrap column to remove the released tag as well as the protease (also His-tagged). The purified untagged *NeuTTM* was recovered in the first fractions.

Crystallization, data collection and structure solution—For crystallographic purposes, the *NeuTTM* gene was expressed as a selenomethionine-substituted protein using standard M9 high yield growth procedure according to the manufacturer's instructions (Shanghai Medicilon; catalog number MD045004-50), with *E. coli* BL21(DE3) codon plus cells.

Crystals for the *NeuTTM* data collection were obtained with hanging drop vapor diffusion using a 24-well Linbro plate. 1 ml of well

solution was added to the reservoir and drops were made with 1 µl of well solution and 1 µl of protein solution. The crystals were grown at 20 °C using 3.5 M sodium formate as a precipitation agent and 0.1 M Bis-Tris propane buffer pH 7.0.

The *NeuTTM* crystal was briefly dipped into a 5-µl drop of cryoprotectant solution (3.8 M sodium formate, 0.2 M NaCl, 4% sucrose, 4% glycerol, 4% ethylene glycol and 0.1 M Bis-Tris propane buffer pH 7.0) before flash-freezing in liquid nitrogen. Data collection was performed at the 19-ID beamline at the Advanced Photon Source, Argonne National Laboratory. One dataset was collected using 0.97959 Å wavelength. Data were indexed and processed with the HKL-2000 package (17).

Intensities were converted into structure factors and 5% of the reflections were flagged for R_{free} calculations using programs F2MTZ, Truncate, CAD and Unique from the CCP4 package of programs (CCP4, 1994). The program BnP (18) was used for the determination of the Se atoms positions and phasing. ARP/wARP package (19) was used to build initial model of the protein. Refinement and manual correction was performed using REFMAC5 (20) version 5.5.0109 and Coot (21) version 0.6. The final model included two protein chains (from residue 4 to residue 153 4-153 in chain A and from residue -1 to residue 153 in chain B), three molecules of ethylene glycol, 8 sodium ions and 324 water molecules. The MOLPROBITY method (22) was used to analyze the Ramachandran plot and root mean square deviations (rmsd) of bond lengths and angles were calculated from ideal values of Engh and Huber stereochemical parameters (23). Wilson B-factor was calculated using CTRUNCATE version 1.0.11 (CCP4, 1994). The figures were created using Pymol (<http://www.pymol.org>). The data collection and refinement statistics are shown in Table 1.

Native Electrospray Mass spectrometry—Electrospray mass spectrometry experiments in native conditions (100 mM ammonium acetate aqueous solution, pH 6.5) were carried out on a Q-TOF Ultima Global mass spectrometer (Waters, Manchester, UK) with the electrospray source in the positive ion mode. The source tuning settings were as follows: capillary = 3 kV, source pirani pressure = 3.3 mbar, cone voltage = 40 V, source temperature = 40 °C, desolvation temperature = 60 °C, collision energy = 10 V. The RF lens 1 voltage was varied from 50 V

(soft conditions to preserve the protein dimer) to 150 V (harder conditions to achieve a better desolvation and higher accuracy in the protein mass determination).

Molecular sieve—A TSK column (G3000SW, 30 x 0.75 cm, 7 mm, Tosoh, Bioscience GmbH, 70567, Stuttgart, Germany) was used in 20 mM HEPES-Na (pH 6.8) and 200 mM NaCl at a flow rate of 0.5 ml/min.

Site-directed mutagenesis of NeuTTM—Point mutations were introduced by the QuickChange method. The expression plasmid containing the coding sequence of NeuTTM was amplified with two mutagenic primers and Pfu DNA polymerase (Promega). Template DNA was removed by digestion with DpnI (Promega) for 2 h at 37 °C. The DNA was then introduced into *E. coli* cells and single clones were isolated. The presence of the mutations was checked by DNA sequencing (Genotranscriptomics Platform, GIGA, University of Liège). The sequences of the oligonucleotides used are given in Supplemental Table S1.

Determination of phosphohydrolase activities—The standard incubation medium (100 µl) contained 50 mM buffer, 5 mM MgCl₂, 0.5 mM PPP_i and 20 µl of the enzyme at the adequate concentration. The mixture was incubated at 37 or 50 °C, the reaction was stopped by addition of 1 ml phosphate reagent (24). The absorbance was read at 635 nm after 30 min and compared with a standard curve to estimate the released inorganic phosphate. When P₄ was the substrate, the absorbance was read after only 15 min, as acid hydrolysis was rapid in the phosphate reagent. The buffers used for incubation at different pH values were: Na-MES (pH 6.0-7.0), Na-MOPS (pH 7.0-7.5), Na-HEPES (pH 7.5-8.0), Na-TAPS (pH 8.0-9.0), Na-CHES (pH 9.0-10.0) and Na-CAPS (pH 10.0-10.5).

Determination of in-gel enzyme activities—In-gel activities were measured as described (25). The gel was colored in phosphate precipitation reagent (1% w/v ammonium heptamolybdate, 1% w/v triethylamine, 1 N HNO₃).

Determination of ATP, ADP and cAMP—Purified NeuTTM was incubated under standard assay conditions with ATP (0.1 mM). The

reaction was stopped by addition of 12% trichloroacetic acid. After extraction of the acid with 3 x 1.5 ml diethyl ether, nucleotides were determined by HPLC using UV detection (26).

Statistical analyses—Data analysis was done with Prism 5 for Mac OS X (GraphPad Software, San Diego, CA) using nonlinear fitting to the Michaelis-Menten equation.

RESULTS

Cloning, overexpression and purification of NeuTTM—The ORF for NeuTTM was subcloned in the pET15b vector, modified to allow the expression of N-terminal His-tag fusion proteins. The latter was purified as described in Materials and Methods. The protein obtained after elution from the HisTrap column was essentially pure as judged by SDS-PAGE (Supplemental Fig. S1). This polyHis fusion protein could be subsequently cleaved by TEV protease, which considerably increased the triphosphatase activity of the enzyme (see below). For crystallization, NeuTTM was expressed as selenomethionine-substituted protein.

Structural properties of NeuTTM—The sequence and secondary structure elements are given in Fig. 1A. Crystallographic data shows that NeuTTM, like 25-kDa ThTPase (9), has an open cleft structure in the absence of bound substrate (Fig. 1B). Several residues projecting into the cleft have been indicated. They seem to be important for substrate and metal binding and/or catalytic activity as, in the case of the closely related CthTTM, extensive mutational analysis (12) has revealed that most of these homologous residues are required for full PPPase activity. Four glutamate residues (E4, E6, E114, E116 and possibly E61 and E63) are supposed to be required for Mg²⁺ (or Mn²⁺) binding while R39 and R41 (and possibly R87) probably interact with substrate phosphoryl groups. According to Keppetipola *et al.* (12), K8, in CthTTM, would form a hydrogen bond with a backbone carbonyl at the break of the C-terminal α4-α5 helix. However, the analysis of the crystal structure of NeuTTM leaves the existence of such a hydrogen bond under question. While the distance between K8NZ and Y142O is 2.9 Å, the angle N...O-C is 117 degrees, which is rather far from the ideal geometry. Also, there is a water molecule (W429) located 3.5 Å away from the Y142 carbonyl oxygen with the angle O...O-C of 172 degrees, which makes this water molecule

a more likely partner for a hydrogen bond with the Y142 carbonyl than K8NZ.

It seems that the β -sheets are prevented from closing into a complete β -barrel by the insertion of a broken C-terminal helix ($\alpha 4$ and $\alpha 5$) into one end of the fold. Such a conformation is stabilized by hydrophobic interactions conferring a relatively rigid structure to *NeuTTM* (Fig. 1C).

Specificity and kinetic properties of recombinant NeuTTM—In contrast to what we expected, only a slight ThTPase activity could be detected, indicating that, unlike its mammalian counterpart, *NeuTTM* is not a genuine ThTPase (Fig. 2).

As ATP and other NTPs were hydrolyzed by a number of enzymes of the TTM family (7,12), we tested these compounds as potential substrates for *NeuTTM*. Nucleoside triphosphatase activity was negligible in the presence of Mg^{2+} , but a small activity was observed in the presence of Mn^{2+} , in particular with GTP (Fig. 2).

By contrast to NTPs, PPP_i was a very good substrate for *NeuTTM* with Mg^{2+} as activator (Fig. 2, Table 2). The enzyme had a strong preference for linear PPP_i compared to cyclic PPP_i (c PPP_i) and to the linear P_4 . The longer chain polyphosphate (containing 65 ± 5 phosphate residues) was not hydrolyzed either. Likewise, guanosine 5'-tetraphosphate (Gpppp or Gp_4), which is a good substrate for *CthTTM* (13), was not significantly hydrolyzed. The *NeuTTM* adenylyl cyclase activity was also checked by incubating the enzyme with ATP plus $MgCl_2$ or $MnCl_2$ at different pH values, but in all cases we did not detect the appearance of a cAMP peak by HPLC. Hence, *NeuTTM* appears to be devoid of adenylyl cyclase activity. Note that the closely related *Clostridium thermocellum* CYTH protein (*CthTTM*) was also devoid of any such activity (12). So far, the only bacterial CYTH proteins with significant (albeit low) adenylyl cyclase activity are the CyaB enzyme AC2 from *A. hydrophila* (4) and the homologous class IV adenylyl cyclase from *Y. pestis* (10,11,27).

General kinetic properties of *NeuTTM* PPPase are displayed in Fig. 3. The optimal temperature was 50-55 °C (Fig. 3A) and the optimum pH was around 9.7 (Fig. 3B). Thermal stability and alkaline pH optimum are characteristic features of several other enzymes of the CYTH superfamily, notably the founding

members CyaB-AC2 (4) and human 25-kDa ThTPase (28).

As Mn^{2+} is a good substituent for Mg^{2+} in several TTM members (7,12,29-31), we tested the possible activating effects of Mn^{2+} ions on *NeuTTM* PPPase activity. We found that it was a very poor substituent for Mg^{2+} at all temperatures tested and in the pH range 7-10 (Fig. 3A, B). However, there was a significant Mn^{2+} -dependent activity at very alkaline pH (10.0-10.5) (Fig. 3B).

Kinetic parameters (K_m , k_{cat} and catalytic efficiency) were determined with different enzyme preparations and under different experimental conditions (Table 2). Using a freshly prepared His-tagged purified preparation, Michaelis-Menten kinetics were obtained (Fig. 3C). At pH 9.7 and 37 °C, K_m was $21 \pm 3 \mu M$ and V_{max} $240 \pm 30 \mu mol \min^{-1} mg^{-1}$ in the presence of 5 mM Mg^{2+} . Under such conditions, the substrate is essentially under the form of a $[Mg^{2+}-PPP_i]$ complex, as K_d for the dissociation of the complex is low ($\sim 1.6 \cdot 10^{-6}$ M). The calculated k_{cat} was $76 s^{-1}$ under these conditions (assuming a molecular mass of 19 kDa for the monomeric enzyme with one catalytic site). The catalytic efficiency of *NeuTTM* triphosphatase activity is thus very high with $k_{cat}/K_m = 3.6 \cdot 10^6 M^{-1}s^{-1}$. At neutral pH, k_{cat}/K_m is about 10 times lower ($3.3 \cdot 10^5 M^{-1}s^{-1}$), but this is still high enough to consider that *NeuTTM* may be a genuine specific inorganic triphosphatase (PPPase). This is all the more plausible as k_{cat} was even higher for the untagged enzyme (up to $7900 s^{-1}$ at 50 °C and pH 9.7, see Table 2). This is two orders of magnitude higher than k_{cat} values obtained for *CthTTM* with its best substrates, PPP_i and Gp_4 (12,13). This raises the possibility that, in *N. europaea*, the physiological function of *NeuTTM* might be the degradation of PPP_i . It should be emphasized, however that any firm conclusion concerning the biological role of this enzyme awaits the demonstration of the presence of inorganic triphosphate in *Nitrosomonas* or any other cell types.

Effects of different activators and inhibitors on recombinant NeuTTM—As their name suggests, enzymes from the TTM family are highly dependent on divalent metal cations. In common with other CYTH enzymes, *NeuTTM* PPPase had an absolute requirement for divalent metal ions, the highest activity being found with Mg^{2+} ions in the concentration range 2-10 mM (Fig. 4A). As already mentioned, Mn^{2+} was less

effective as an activator (Fig. 4A), but half-maximum activation was obtained at 0.4 mM Mn^{2+} , which corresponds to a very low concentration of free Mn^{2+} .

We also tested the activating effect of Co^{2+} , which, like Mn^{2+} , is a good activator for several TTM enzymes (30). At optimal pH (9.5-9.7), Co^{2+} was a better activator than Mn^{2+} , though the maximum activity was less than 10% of the one measured in the presence of 5 mM Mg^{2+} (Fig. 4B). The concentration of free Co^{2+} corresponding to half-maximum activation was extremely low (about 30-50 nM), indicating that the affinity of the binding site for Co^{2+} is even higher than for Mn^{2+} .

As already reported for other CYTH enzymes such as Cet1 (30) and 25-kDa ThTPase (28), Ca^{2+} had no activating effect, but it was a potent inhibitor in the presence of Mg^{2+} (Fig. 5A): IC_{50} was 50-100 μM in the presence of 5 mM Mg^{2+} . Mn^{2+} was also a potent inhibitor in the presence of Mg^{2+} , at least at pH < 10 (IC_{50} ~40 μM). As Mn^{2+} is also a weak activator, the inhibition by Mn^{2+} in the presence of Mg^{2+} was not complete. The curves showing the activating effect of increasing concentrations of Mg^{2+} were shifted to the right in the presence of Ca^{2+} (Fig. 5B), suggesting that the latter ion exerts its inhibitory effect, at least partially, by competition with Mg^{2+} . We finally tested the effect of Zn^{2+} , which has been shown to be a potent inhibitor of mammalian 25-kDa ThTPase (28). Zn^{2+} inhibited *Neu*TTM PPPase in the lower micromolar range (IC_{50} ~1.5 μM) (Fig. 5C). In contrast to Ca^{2+} , the inhibitory effect of Zn^{2+} was only marginally affected by the concentration of the activator Mg^{2+} (data not shown), suggesting that the two cations do not compete for the same binding site. This was also the case for 25-kDa ThTPase (28). Those data are in agreement with the assumption that Mg^{2+} , Mn^{2+} , Ca^{2+} and Co^{2+} may share a common binding site, while Zn^{2+} may bind to a peripheral “allosteric” site.

In addition to Zn^{2+} , Cd^{2+} and Cu^{2+} ions were also inhibitory but with higher IC_{50} values, 10 and 20 μM respectively.

Structural and binding properties of the NeuTTM protein analyzed by native mass spectrometry—We first investigated the ability of the 19-kDa recombinant *Neu*TTM to dimerize in solution. The X-ray diffraction data already suggested that the protein crystallized as a dimer (14). We carried out electrospray mass spectrometry of the concentrated His-tagged

protein (total monomer concentration 10 μM) in 100 mM ammonium acetate, pH 6.5 (Fig. 6) and found that the protein was a mixture of monomer (noted M) and dimer (noted M_2) forms, the dimer being more abundant. The dimer dissociated easily in the gas phase when the RF lens 1 voltage was increased from 50 V to 150 V. This suggests that salt bridge interactions are not prevailing at the dimerization interface. Indeed, the diffraction data show that the interface is mainly composed of hydrophobic amino acids, among which are L29, L38, L40, L51, L74, I36, I64 and I66 (Supplemental Fig. S2), and this explains the lability of the dimers in electrospray.

We then studied the complexes of *Neu*TTM, with substrates alone (PPP_i, ATP and ThTP) in the presence of Mg^{2+} . In all cases, the substrates remained tightly bound to *Neu*TTM at all voltages, in line with ionic interactions in these complexes. Fig. 7 shows the mass spectra of *Neu*TTM alone (Fig. 7A), and of the binary mixture of with PPP_i (Fig. 7B), ATP (Fig. 7C) and ThTP (Fig. 7D). With PPP_i, at the concentrations used (10 μM *Neu*TTM and 25 μM PPP_i), the peak of the free protein is not distinguishable from the noise. It can therefore be estimated that the concentration of free protein is less than 8.5% of the total protein concentration. This means that the dissociation constant for the monomer-substrate complex under conditions stated above must be lower than 1.5 μM . Moreover, the protein dimers contain exclusively two PPP_i molecules, as seen from the uneven charge states 15+ and 13+. This strongly contrasts with ATP and ThTP, where the free protein is predominant, and both the monomer and dimer bind one molecule of substrate on average. From the peak intensities, the K_d of the monomer-substrate complex is estimated to be at least 90 μM for ATP and ThTP. This is in agreement with the high K_m value ($800 \pm 120 \mu\text{M}$) measured for ATPase activity of *Neu*TTM (Table 2).

Figure 8 shows the mass spectra of charge state 8+ of the protein monomer in different mixtures with Mg^{2+} and/or PPP_i. The protein alone shows a peak at $m/z = 2499.4$ (Fig. 8A), that remains predominant when the protein is mixed with a 10-fold excess of Mg^{2+} (Fig. 8B). We found that both monomers and dimers bind Mg^{2+} with moderate affinity. We also tested binary mixtures of the protein with Mn^{2+} and Zn^{2+} , and the results suggest a higher affinity for Zn^{2+} (with multiple binding sites) than for Mg^{2+}

and Mn^{2+} (data not shown). This is in agreement with the finding that the PPPase activity of *NeuTTM* is inhibited by micromolar concentrations of Zn^{2+} (Fig. 5C).

A more detailed analysis of the masses of the [*NeuTTM*- PPP_i] complexes in the absence of divalent cations revealed that they specifically take up two monovalent cations (the peak intensities of the complexes with zero and one monovalent cations being insignificant). Data from Fig. 8C show the presence of a complex with two Na^+ ions. The latter presumably originate from the tripolyphosphate preparation, which is in the form of a pentasodium salt. A [*NeuTTM*- PPP_i - Na^+ - K^+] complex was also detected, with K^+ possibly originating from the protein preparation.

Finally, we investigated the properties of the ternary complexes (supposed to be catalytically active) of *NeuTTM*, with the substrate PPP_i and the activator Mg^{2+} . In order to avoid appreciable hydrolysis of PPP_i , the spectra were recorded immediately after mixing the protein with Mg^{2+} and PPP_i . In spite of the high enzyme concentration, PPPase activity is low at room temperature and pH 6.5 (see Fig. 3) and complete hydrolysis of PPP_i under the present conditions would probably take more than a few seconds. With $MgCl_2$ (0.1 mM) in addition to PPP_i , the [enzyme- PPP_i] complex took up one Mg^{2+} ion rather than two monovalent cations (Fig. 8D). No free enzyme was observed. We can therefore assume that the [Mg - PPP_i] complex (which is the true substrate) binds to the active site with high affinity, K_d being of the same order of magnitude than for free PPP_i (<1.5 μM).

On the other hand, it is clear that the requirement for an activating Mg^{2+} ion is not simply due to the fact that it binds to PPP_i . Although the true substrate is likely to be the [Mg^{2+} - PPP_i] complex, the divalent metal activator must also bind to a specific site on the protein, as full enzyme activity requires the presence of millimolar free Mg^{2+} in the incubation medium (Fig. 4A and 5B) This was also shown to be the case for RNA triphosphatase from *Trypanosoma* (29) and it is probably a general feature of CYTH proteins (3). In the case of *NeuTTM*, the metal ion presumably interacts with the carboxyl groups of Glu4, Glu6, Glu114 and Glu116 (see Fig. 1).

There is no evidence from the present data that the protein might bind more than one Mg^{2+} ion with appreciable affinity. The same

conclusion was reached by Song et al. (9) for the 25-kDa mouse ThTPase. Although Iyer and Aravind (3) suggested that CYTH proteins may bind two divalent metal activators, this is probably not a general rule for this superfamily of proteins.

In-gel activity of NeuTTM under non-denaturing conditions—In agreement with mass spectrometric data, two peaks of approximately 20 and 40 kDa were obtained after separation on a size exclusion column (Supplemental Fig. S3). The specific activities of the monomer and the dimer were respectively 245 and 169 $\mu mol \cdot min^{-1} \cdot mg^{-1}$ with 0.5 mM PPP_i at 50 °C, suggesting that the catalytic activity was not much changed by dimerization. This was also confirmed by in-gel activity determination after polyacrylamide gel electrophoresis under non-denaturing conditions and incubation under optimal conditions (Supplemental Fig. S4). Furthermore, when the monomer and the dimer were separated on the size exclusion column and then reinjected, both appeared pure, suggesting that no rapid conversion between the two forms occurs. These results suggest that dimerization may simply be an artifact associated with enzyme purification and without physiological significance.

Site-directed mutagenesis—Alanine mutation of K8 and K85 were chosen because homologous residues were reported to be important for catalytic activity and substrate specificity of the closely related *CthTTM* (12). Indeed, the primary structures of *CthTTM* and *NeuTTM* have 73 positions of side-chain identity (12).

We found that, in contrast to the K8A mutant of *CthTTM*, the K8A mutated *NeuTTM* remained highly active with PPP_i as substrate and Mg^{2+} as activator, with a catalytic efficiency close to that of the recombinant wild-type enzyme, as both K_m and k_{cat} were increased (Table 2). This is an important difference with *CthTTM*. Indeed, Keppetipola *et al.* (12) found that the corresponding K8A mutation in *CthTTM* nearly completely abolished the PPPase activity of the enzyme, while strongly stimulating its ATPase activity. According to (12), K8 would form a hydrogen bond with a backbone carbonyl at the break of the C-terminal helices $\alpha 4$ - $\alpha 5$, stabilizing the open structure of the eight-stranded β -barrel where the substrate binds. Substituting K8 by alanine would prevent this specific interaction between the $\beta 1$ strand and $\alpha 4$ - $\alpha 5$ helices, making the conformation less

rigid. Our own data do not suggest that such a H-bond is required to maintain a rigid structure. Furthermore, with the mutated K8A enzyme, ATP remains a poor substrate (Table 2), even with Mn^{2+} as activator, the catalytic efficiency being 3 orders of magnitude lower than with PPP_i . The present results suggest that either a very rigid conformation is not essential for a high and specific PPPase activity of *NeuTTM* or that K8 is not involved in the stabilization of the enzyme conformation. Note that Keppetipola *et al.* (12) made their assumption on the basis of sequence similarities with *NeuTTM*, and that the three-dimensional structure of *CthTTM* is not known.

K85 is located at the bottom of the cleft that is supposed to contain the catalytic site, close to the arginine residues (R39, R41 and R87) that are thought to bind the substrate phosphoryl groups electrostatically. In the case of the very similar *CthTTM* protein, the K87 residue, which is homologous to K85 in *NeuTTM*, has been found to be essential for catalysis, but the authors did not determine K_m and V_{max} (12).

The K85A mutant of *NeuTTM* was about ten times less active than the non-mutated enzyme, but the optimal conditions for activity were essentially the same, *i. e.* pH 9.7, temperature ~ 50 °C. The mutant was also much less active with ATP than with PPP_i as substrate. The extrapolated V_{max} value yielded a k_{cat} around 21 s^{-1} (at 50 °C) in the presence of 5 mM Mg^{2+} (Table 2), which is 14 times lower than k_{cat} measured under the same optimal conditions for the non-mutated enzyme. On the other hand, the K_m for PPP_i was 1 or 2 orders of magnitude higher than for the non-mutated *NeuTTM*. Note that due to the high K_m , it was not possible to use saturating substrate concentrations, increasing the uncertainty on both K_m and V_{max} . While the catalytic efficiency of the enzyme appears to be rather strongly decreased by the K85A mutation, it cannot be concluded that K85 is really essential for catalysis as k_{cat} remains relatively high.

Another important consequence of the K85A mutation is that the effects of divalent cations are profoundly altered: in contrast to the non-mutated enzyme, the K85A mutant is more strongly activated by Mn^{2+} than by Mg^{2+} and the inhibitory effects of Ca^{2+} and Zn^{2+} are less pronounced (Supplemental Table S2). Actually, Zn^{2+} can even replace Mn^{2+} as activator, though it is less effective. It thus appears that deleting the positive charge of the side chain at position

85 alters the protein conformation in such a way that cations larger than Mg^{2+} become better activators. This suggests that K85 may act as a “discriminator” residue, ensuring that the smaller and more physiological Mg^{2+} ion is the specific activator. Taken together the data suggest that K85 is not directly involved in catalysis and is more likely to play an important (though not essential) role to properly orient the PPP_i molecule in the enzyme-substrate complex. It is also important for the specificity of Mg^{2+} binding.

As neither K8 nor K85 appear to be essential residues for catalysis, we suspected that K52, which is highly conserved in CYTH proteins (3,9), might play a more essential role. In *CthTTM*, mutation of K52 resulted in the loss of 90 to 99% of the activity, depending on the substrate or activator used (12). In *NeuTTM*, the conservative K52R mutation resulted in a decreased V_{max} by about two orders of magnitude (Table 2) and, as the apparent K_m is strongly increased (Supplemental Table S5), the catalytic efficiency is at least 1000 times lower than that of the non-mutated enzyme. Mn^{2+} did not induce a significant activation of this mutant. Thus, in contrast to K85A, the specificity for activating ions does not appear to be changed.

The fact that this conservative mutation strongly decreases the catalytic efficiency of the enzyme suggests that this highly conserved lysine residue plays an important role in the catalytic mechanism.

A puzzling property of *NeuTTM*, as well as other enzymes of the CYTH protein family, is their strong activation at alkaline pH (Fig. 3B). In order to check that this pH profile was not due to impaired binding of the substrate at lower pH, we plotted V_{max}/K_m as a function of pH (Fig. 9A). Our results show that the K_m does not change much with pH and the profile obtained is quite similar to the activity *versus* pH profile (Fig. 3B). We used the Dixon-Webb plot $\text{Log } V_{max}$ *versus* pH to estimate the pK_a value for the main residue responsible for activity decrease between 9.7 and 7.0. As shown in Fig. 9B, the estimated pK_a was close to 9.3 for the non-mutated enzyme. The same value was found for the K52R mutant. These data are in agreement with the proposal that the catalytic activity depends on a single deprotonation step with $pK_a \sim 9.3$. This may correspond to a general base that removes a proton from water; the resulting OH^- would attack a phosphorus atom of the PPP_i substrate.

As the pH-rate profile remains largely unaffected by K52R mutation, the decrease of activity between 9.7 and 7.0 cannot be ascribed to protonation of the K52 amino group. This suggests the involvement of another residue able to interact with K52 and acting as a general base in the hydrolytic mechanism. According to the crystal structure (Fig. 1B), only three residues are in a position to interact easily with K52: Y28, E37 and E61 (see also supplemental Fig. S6). Obviously, the carboxyl groups of glutamate residues could hardly exhibit such an alkaline pK_a and we suspected that the residue acting as the general base was Y28 (pK_a for the hydroxyl group of free tyrosine is ~ 10.0). Indeed, the conservative mutation Y28F results in a strong loss of enzyme activity ($\sim 2.6 \mu\text{mol min}^{-1} \text{mg}^{-1}$ at $100 \mu\text{M PPP}_i$, compared to $\sim 200 \mu\text{mol min}^{-1} \text{mg}^{-1}$ for the non-mutated enzyme, Fig. 3C). Surprisingly, however, the activity continuously increased when $[\text{PPP}_i]$ was raised up to 1 mM (the highest testable concentration with our method) with no tendency to saturation (Supplemental Fig. S5). This lack of saturation was observed at all pH values tested from 7.0 to 0.9 (data not shown). Thus, the kinetic parameters K_m and V_{max} could not be estimated with this mutant enzyme. The pH optimum of the Y28F mutant is shifted to lower values compared to the non-mutated (Fig. 3B) and the K52R mutant (Fig. 9C). We plotted the Log of the specific activity versus pH at 37°C for $[\text{PPP}_i] = 100 \mu\text{M}$ (Fig. 9D). It is obvious that there is an important shift in pH-rate profile towards lower pH values and the Dixon-Webb plot yielded a pK_a value ~ 7.4 . This apparent pK_a was not strongly affected by changes in PPP_i concentration (not shown).

This value might possibly reflect the pK_a of the carboxyl group of a neighboring glutamate (E37 or E61) that might also act as a general base, albeit less efficiently than Y28. This would explain that the activity of the Y28F mutant still reaches relatively high values when PPP_i is in large excess (Supplemental Fig. S5).

Taken together, those data suggest that Y28 plays an important role in *NeuTTM* catalysis (possibly forming a catalytic dyad with K52) and is, at least partially, responsible for the unusual high pH optimum of the enzyme.

The relatively slight decrease in activity at $\text{pH} \geq 10$ could result from a number of possibilities, *e. g.* charge alterations involving unidentified residues in or near the active site, or destabilization of the protein structure.

In the model shown in Fig. 10, we hypothesize that a catalytic dyad is formed by the Y28-K52 pair, the nucleophilic nitrogen of K52 being hydrogen-bonded with the phenolate oxygen of Y28. The latter would act as the general base that removes a proton from water and the resulting OH^- attacks a phosphorus atom of the substrate PPP_i (Fig. 10A). Alternatively, Y28 might act as a nucleophile to directly attack the γ -phosphorus atom of PPP_i (Fig. 10B). In the latter case, we would expect a covalent phosphotyrosyl intermediate to be formed, which would be unusual for a hydrolase. When the catalytic mechanism involves a phosphoenzyme intermediate, the activity is generally inhibited by sodium orthovanadate acting as a transition state inhibitor. We tested the effect of sodium orthovanadate on the non-mutated *NeuTTM* PPPase activity, but we found no inhibition at concentrations up to 2 mM. However, the activity was very sensitive to fluoride with an IC_{50} as low as $30 \pm 10 \mu\text{M}$ for NaF (results not shown). Fluoride is a well-known inhibitor of acid phosphatases, but millimolar concentrations are required. However, inorganic pyrophosphatases are sensitive to fluoride at concentrations lower than 1 mM. In family I pyrophosphatases, where fluoride inhibition involves rapid and slow phases (32), there is much evidence that catalysis proceeds by direct phosphoryl transfer to water rather than via a phosphoryl enzyme intermediate (33,34). The structure of the F^- -inhibited complex has shown a fluoride ion replacing the nucleophilic water molecule (35). In family II pyrophosphatases, which belong to the DHH phosphoesterase superfamily (as defined by (5)), the IC_{50} for fluoride inhibition was even lower than for *NeuTTM* ($\sim 12 \mu\text{M}$) (36). In any case, fluoride is believed to act as an analogue of hydroxide (37). The detailed mechanism of PPP_i hydrolysis by *NeuTTM* requires further investigation, but the lack of effect of vanadate and the strong inhibitory effect of fluoride argue against the existence of a covalent phosphoenzyme intermediate. Therefore, the model proposed in Fig. 10 seems to be the simplest and the most plausible.

DISCUSSION

The present data demonstrate that the hypothetical protein NE1496, present in *N. europaea* (*NeuTTM*), is a functional phosphohydrolase with surprisingly high specificity, affinity and catalytic efficiency for

PPP_i. This is also the first molecular characterization of a specific tripolyphosphatase. Several enzymes hydrolyzing PPP_i have been characterized previously, but they are mainly exopolyphosphatases that, in addition to PPP_i, hydrolyze other substrates such as, for instance, long chain polyphosphates or Gp₄ (38-40). So far, only one enzyme was reported to be strictly specific for PPP_i hydrolysis: it was purified from *N. crassa* and found to be a dimer of 40 kDa subunits (41). Its sequence remains unknown and, unlike *NeuTTM*, it does not appear to have a high affinity for PPP_i.

NeuTTM belongs to the superfamily of CYTH proteins (3) and was first referred to as a hypothetical protein with putative phosphatase or CyaB-like adenylyl cyclase activity by analogy with the *A. hydrophila* CYTH protein (4). However, it has become clear that the functional properties of CYTH proteins cannot be predicted from primary or even three-dimensional structure. In fact, the CYTH domain is a functionally versatile protein fold, characterized mainly by its ability to bind triphosphate compounds and catalyze their hydrolysis or other chemical transformations in the presence of divalent metal ion activators. Members of the CYTH superfamily exist in archaea, but none has been functionally characterized so far. In bacteria, two CYTH orthologs were shown to have an adenylyl cyclase activity (4,11,27) but, under physiological conditions, this activity is low and its biological significance is not established. *CthTTM*, the ortholog from *C. thermocellum* hydrolyzes PPP_i with a relatively good turnover ($k_{\text{cat}} = 3 \text{ s}^{-1}$), but it also hydrolyzes other substrates such as Gp₄ ($k_{\text{cat}} = 96 \text{ s}^{-1}$) and, to a lesser extent, nucleoside triphosphates and long chain polyphosphates. (12,13). Thus, its possible physiological function remains undefined. In contrast, a clear biological role has been demonstrated for the CYTH orthologs of fungi and protozoa, which catalyze the first step of RNA capping in these organisms (7). In pluricellular eukaryotes, only the mammalian 25-kDa ThTPase has been characterized (1,9,28). Like *NeuTTM*, the latter enzyme is characterized by a high specificity and a high catalytic efficiency ($k_{\text{cat}}/K_m = 6 \cdot 10^6 \text{ M}^{-1} \text{ s}^{-1}$ for the bovine ThTPase (1)). On the basis that all known CYTH proteins hydrolyze triphosphates and that PPP_i is the simplest triphosphate compound conceivable, PPPase activity might well be the primitive enzymatic activity in the CYTH protein family, which later evolved to hydrolyze more complex

organic substrates such as RNA or ThTP in eukaryotes.

It should be pointed out that a high affinity for PPP_i was already demonstrated in the case of yeast RNA triphosphatases, where PPP_i is a potent competitive inhibitor, albeit a poor substrate (29,42,43).

The present data show that, despite low sequence similarity and profound structural differences, *NeuTTM* and 25-kDa ThTPase have several kinetic properties in common, *i. e.* requirement for Mg²⁺, inhibition by Ca²⁺ by competition with Mg²⁺, allosteric inhibition by Zn²⁺, alkaline pH optimum and an optimal temperature around 50-60 °C. *A. hydrophila* and *Y. pestis* CyaB-like adenylyl cyclases are also Mg²⁺-dependent and have high pH and temperature optima (4,11,27). Although more detailed investigations are required, most of these features may possibly be functional signature properties of CYTH enzymes.

Our results shed some light on the particular conformation of the *NeuTTM* protein and the relationship between structural and kinetic properties of the enzyme. The open cleft structure (incomplete β-barrel) is in contrast to the closed tunnel conformation of other TTM proteins (7). It appears to be rather rigid and to be stabilized by hydrophobic interactions between the antiparallel β strands and the broken C-terminal α4-α5 helix (Fig. 1C). Hence, in contrast to mammalian 25-kDa ThTPase (9), *NeuTTM* is probably unable to form a tunnel-like structure, even when a substrate is bound. This is in line with the very different substrate specificities of the two enzymes.

We propose a catalytic mechanism (Fig. 10) in which the hydroxyl group of Y28 hydrogen-bonded to the nucleophilic nitrogen of K52 acts as a nucleophile, attacking a water molecule to form OH⁻. K52 was also considered essential in the enzymatic activity of *CthTTM* (12).

To our knowledge, this is the first lysine-tyrosine dyad proposed for a hydrolase. Such a mechanism strongly contrasts with the classical serine-histidine dyad observed in many phosphatases.

Catalytic dyads based on tyrosyl and lysyl residues seem to be rare (44), nevertheless such a catalytic dyad has been suggested for the enol-keto tautomerization step of the NADP⁺-dependent malic enzyme (45). In that enzyme, the K→R and Y→F mutations resulted in a decrease in k_{cat} by two orders of magnitude as we observed here.

In the crystal structure described here, the distance between K52 and Y28 is 7.4 Å (Supplemental Fig. S6), too much for a hydrogen bond between these two residues. However, as shown for ThTPase, the binding of the substrate induces an important conformational change (9). Such a conformational change in *NeuTTM* might bring the two residues close enough for an interaction.

Four glutamate residues, E4, E6, E114 and E116 protrude from the bottom into the catalytic cleft. They are part of the CYTH consensus sequence and are thought to be involved in Mg^{2+} binding (3,12). Our data show that the enzyme substrate complex binds only one Mg^{2+} ion (Fig. 8B). We may thus consider the possibility that this Mg^{2+} , as well as probably K85, stabilize and orient the substrate PPP_i towards the catalytic dyad projecting from the ceiling of the cleft (Fig. 1B).

Concerning the quaternary structure, it is worth pointing out that *NeuTTM* crystallizes as a dimer (14) and can also form dimers in solution. However, our results suggest that dimerization is probably not of physiological significance for *NeuTTM*. This is in contrast to yeast RNA triphosphatases Cet1 from *S. cerevisiae* and Pet1 from *Schizosaccharomyces pombe*, where dimerization is important for thermal stability and *in vivo* function (46).

The high affinity and specificity of *NeuTTM* for PPP_i raises the question of the possible biological roles of both PPP_i and the enzymes able to synthesize it. For PPP_i , there are so far very few data concerning its enzymatic synthesis. In *E. coli*, it was shown long ago that PPP_i can be produced by enzymatic cleavage of deoxyguanosine triphosphate (47). On the other hand, it is well known that PPP_i is formed as an intermediate in the enzymatic synthesis of S-adenosylmethionine but, in this case, it is not released in the cytosol (48). It was also shown that PPP_i is an intermediate in naturally occurring pterins in *Drosophila melanogaster* (49).

Like ThTP (50), PPP_i was shown to be an alternative phosphate donor for protein phosphorylation *in vitro* (51) and therefore, like

cAMP and possibly ThTP (15), PPP_i might act as an intracellular signal.

However, in contrast to inorganic polyP of higher molecular weight (>10 phosphoryl residues), PPP_i and other very short chain polyphosphates have never been reported to exist in any organism (except in acidocalcisomes, specific organelles rich in calcium and polyphosphates in some protozoans (52)). In all likelihood, this is simply due to the present lack of sensitive and specific detection methods. For polyphosphates of longer chain (15-750 residues), the problem was overcome thanks to sensitive assay methods (53). In *E. coli*, polyphosphates play an important role in the response to various forms of environmental stress (54-56). Polyphosphates may also act as energy stores or divalent cation chelators (56). The demonstration of similar physiological roles for PPP_i awaits the development of an adequate method to measure its intracellular concentration.

Hence, the present results provide the first detailed characterization of a specific PPP_i ase with high affinity for PPP_i and high catalytic efficiency. Although, it is not proven that the physiological function of the protein is to degrade PPP_i *in vivo*, our study is a first step towards the understanding of the possible roles of short chain polyphosphates, which might turn out to be just as important as their long chain counterparts in cell biology.

Acknowledgements—Nucleic acid sequencing was performed by Véronique Dhennin, Genotranscriptomics Platform, GIGA, University of Liège, <http://www.giga.ulg.ac.be/>. We thank Dr. Eric Oldfield for the gift of tetrapolyphosphate and Dr. Ilca Margineanu for help with the manuscript and some experiments. We are grateful to Dr. Alexei Savchenko for the gift of the pET15b vector for the expression of *NeuTTM* and helpful discussion. The structure of *NeuTTM* was determined by the Midwest Centre for Structural Genomics as part of NIH Protein Structure Initiative (Grants GM074942).

REFERENCES

1. Lakaye, B., Makarchikov, A. F., Antunes, A. F., Zorzi, W., Coumans, B., De Pauw, E., Wins, P., Grisar, T., and Bettendorff, L. (2002) *J. Biol. Chem.* **277**, 13771-13777
2. Gangolf, M., Czerniecki, J., Radermecker, M., Detry, O., Nisolle, M., Jouan, C., Martin, D., Chantraine, F., Lakaye, B., Wins, P., Grisar, T., and Bettendorff, L. (2010) *PLoS One* **5**, e13616

3. Iyer, L. M., and Aravind, L. (2002) *BMC Genomics* **3**, 33
4. Sismeiro, O., Trotot, P., Biville, F., Vivares, C., and Danchin, A. (1998) *J. Bacteriol.* **180**, 3339-3344
5. Aravind, L., and Koonin, E. V. (1998) *Trends Biochem. Sci.* **23**, 17-19
6. Tesmer, J. J., Sunahara, R. K., Johnson, R. A., Gosselin, G., Gilman, A. G., and Sprang, S. R. (1999) *Science* **285**, 756-760
7. Gong, C., Smith, P., and Shuman, S. (2006) *RNA* **12**, 1468-1474
8. Lima, C. D., Wang, L. K., and Shuman, S. (1999) *Cell* **99**, 533-543
9. Song, J., Bettendorff, L., Tonelli, M., and Markley, J. L. (2008) *J. Biol. Chem.* **283**, 10939-10948
10. Gallagher, D. T., Smith, N. N., Kim, S. K., Heroux, A., Robinson, H., and Reddy, P. T. (2006) *J. Mol. Biol.* **362**, 114-122
11. Gallagher, D. T., Kim, S. K., Robinson, H., and Reddy, P. T. (2011) *J. Mol. Biol.* **405**, 787-803
12. Keppetipola, N., Jain, R., and Shuman, S. (2007) *J. Biol. Chem.* **282**, 11941-11949
13. Jain, R., and Shuman, S. (2008) *J. Biol. Chem.* **283**, 31047-31057
14. Lunin, V. V., Skarina, T., Onopriyenko, O., Binkowski, T. A., Joachimiak, A., Edwards, A. M., and Savchenko, A. (2005) *Protein Data Bank 2FBL*
15. Lakaye, B., Wirtzfeld, B., Wins, P., Grisar, T., and Bettendorff, L. (2004) *J. Biol. Chem.* **279**, 17142-17147
16. Bettendorff, L., Nghiêm, H. O., Wins, P., and Lakaye, B. (2003) *Anal. Biochem.* **322**, 190-197
17. Otwinowski, Z., and Minor, W. (1997) Processing of X-ray Diffraction Data Collected in Oscillation Mode. in *Methods in Enzymology* (Carter, C. W., Jr, and Sweet, R. M. eds.), Academic Press, New York
18. Weeks, C. M., Shah, N., Green, M. L., and Miller, R. (2005) *Acta Cryst.* **A61**, C152
19. Cohen, S. X., Morris, R. J., Fernandez, F. J., Ben Jelloul, M., Kakaris, M., Parthasarathy, V., Lamzin, V. S., Kleywegt, G. J., and Perrakis, A. (2004) *Acta Crystallogr. D Biol. Crystallogr.* **60**, 2222-2229
20. Murshudov, G. N., Vagin, A. A., and Dodson, E. J. (1997) *Acta Cryst.* **D53**, 240-255
21. Emsley, P., and Cowtan, K. (2004) *Acta Cryst.* **D60**, 2126-2132
22. Lovell, S. C., Davis, I. W., Arendall, W. B., 3rd, de Bakker, P. I., Word, J. M., Prisant, M. G., Richardson, J. S., and Richardson, D. C. (2003) *Proteins* **50**, 437-450
23. Engh, R. A., and Huber, R. (1991) *Acta Cryst.* **A47**, 193-400
24. Lanzetta, P. A., Alvarez, L. J., Reinach, P. S., and Candia, O. A. (1979) *Anal. Biochem.* **100**, 95-97
25. Simonovic, A. D., Gaddameedhi, S., and Anderson, M. D. (2004) *Anal. Biochem.* **334**, 312-317
26. Hill, M., Dupaix, A., Volfín, P., Kurkdian, A., and Arrio, B. (1987) *Meth. Enzymol.* **148**, 132-141
27. Smith, N., Kim, S. K., Reddy, P. T., and Gallagher, D. T. (2006) *Acta Crystallogr. Sect. F Struct. Biol. Cryst. Commun.* **62**, 200-204
28. Lakaye, B., Makarchikov, A. F., Wins, P., Margineanu, I., Roland, S., Lins, L., Aichour, R., Lebeau, L., El Moualij, B., Zorzi, W., Coumans, B., Grisar, T., and Bettendorff, L. (2004) *Int. J. Biochem. Cell. Biol.* **36**, 1348-1364
29. Gong, C., Martins, A., and Shuman, S. (2003) *J. Biol. Chem.* **278**, 50843-50852
30. Ho, C. K., Pei, Y., and Shuman, S. (1998) *J. Biol. Chem.* **273**, 34151-34156
31. Bisailon, M., and Shuman, S. (2001) *J. Biol. Chem.* **276**, 17261-17266
32. Baykov, A. A., Fabrichniy, I. P., Pohjanjoki, P., Zyryanov, A. B., and Lahti, R. (2000) *Biochemistry* **39**, 11939-11947
33. Gonzalez, M. A., Webb, M. R., Welsh, K. M., and Cooperman, B. S. (1984) *Biochemistry* **23**, 797-801
34. Zyryanov, A. B., Pohjanjoki, P., Kasho, V. N., Shestakov, A. S., Goldman, A., Lahti, R., and Baykov, A. A. (2001) *J. Biol. Chem.* **276**, 17629-17634
35. Heikinheimo, P., Tuominen, V., Ahonen, A. K., Teplyakov, A., Cooperman, B. S., Baykov, A. A., Lahti, R., and Goldman, A. (2001) *Proc. Natl. Acad. Sci. U S A* **98**, 3121-3126
36. Fabrichniy, I. P., Lehtio, L., Tammenkoski, M., Zyryanov, A. B., Oksanen, E., Baykov, A. A., Lahti, R., and Goldman, A. (2007) *J. Biol. Chem.* **282**, 1422-1431
37. Briley, P. A., Eisenthal, R., and Harrison, R. (1975) *Biochem. J.* **145**, 501-507
38. Wurst, H., and Kornberg, A. (1994) *J Biol. Chem.* **269**, 10996-11001

39. Fang, J., Ruiz, F. A., Docampo, M., Luo, S., Rodrigues, J. C., Motta, L. S., Rohloff, P., and Docampo, R. (2007) *J. Biol. Chem.* **282**, 32501-32510
40. Tammenkoski, M., Koivula, K., Cusanelli, E., Zollo, M., Steegborn, C., Baykov, A. A., and Lahti, R. (2008) *Biochemistry* **47**, 9707-9713
41. Egorov, S. N., and Kulaev, I. S. (1976) *Biokhimiya* **41**, 1958-1967
42. Gong, C., and Shuman, S. (2002) *J. Biol. Chem.* **277**, 15317-15324
43. Issur, M., Despins, S., Bougie, I., and Bisailon, M. (2009) *Nucleic Acids Res.* **37**, 3714-3722
44. Gutteridge, A., and Thornton, J. M. (2005) *Trends Biochem. Sci.* **30**, 622-629
45. Kuo, C. C., Lin, K. Y., Hsu, Y. J., Lin, S. Y., Lin, Y. T., Chang, G. G., and Chou, W. Y. (2008) *Biochem. J.* **411**, 467-473
46. Hausmann, S., Pei, Y., and Shuman, S. (2003) *J. Biol. Chem.* **278**, 30487-30496
47. Kornberg, S. R., Lehman, I. R., Bessman, M. J., Simms, E. S., and Kornberg, A. (1958) *J. Biol. Chem.* **233**, 159-162
48. Perez Mato, I., Sanchez del Pino, M. M., Chamberlin, M. E., Mudd, S. H., Mato, J. M., and Corrales, F. J. (2001) *J. Biol. Chem.* **276**, 13803-13809
49. Switchenko, A. C., Primus, J. P., and Brown, G. M. (1984) *Biochem. Biophys. Res. Commun.* **120**, 754-760
50. Nghiêm, H. O., Bettendorff, L., and Changeux, J. P. (2000) *FASEB J.* **14**, 543-554
51. Tsutsui, K. (1986) *J. Biol. Chem.* **261**, 2645-2653
52. Moreno, B., Urbina, J. A., Oldfield, E., Bailey, B. N., Rodrigues, C. O., and Docampo, R. (2000) *J. Biol. Chem.* **275**, 28356-28362
53. Ault-Riche, D., Fraley, C. D., Tzeng, C. M., and Kornberg, A. (1998) *J. Bacteriol.* **180**, 1841-1847
54. Kuroda, A., Nomura, K., Ohtomo, R., Kato, J., Ikeda, T., Takiguchi, N., Ohtake, H., and Kornberg, A. (2001) *Science* **293**, 705-708
55. Brown, M. R., and Kornberg, A. (2008) *Trends. Biochem. Sci.* **33**, 284-290
56. Rao, N. N., Gomez-Garcia, M. R., and Kornberg, A. (2009) *Annu. Rev. Biochem.* **78**, 605-647

FOOTNOTES

* This study was supported by grants 2.4558.04 and 2.4508.10 from the “Fonds de la Recherche Fondamentale Collective” (FRFC) of the F.R.S.-FNRS to Lucien Bettendorff, Edwin De Pauw, and Bernard Lakaye and the NIH Protein Structure Initiative (Grant P50-GM62413-02) to Dr. Alexei Savchenko (Banting and Best Department of Medical Research, University of Toronto, Toronto, Ontario, M5G 1L6, Canada).

¹ Research Fellow of the Fonds pour la formation à la Recherche dans l’Industrie et dans l’Agriculture (FRIA).

² Present address : National Centre for Mass Spectrometry, Indian Institute of Chemical Technology, Uppal Road, Tarnaka, Hyderabad-500607, India.

³ Research Associates of the Fonds de la Recherche Scientifique – FNRS.

⁴ Present address : Biosciences Center, National Renewable Energy Laboratory, 1617 Cole Blvd. MS 3323 Golden, CO 80401.

⁵ Research Director of the Fonds de la Recherche Scientifique – FNRS.

⁶ Abbreviations: AC, adenylyl cyclase; cPPP_i, cyclic trimetaphosphate; Gp₄, guanosine 5'-tetrakisphosphate; NTP, nucleoside triphosphate; P₄, inorganic tetraphosphate, PolyP, inorganic polyphosphate; PPPase, inorganic triphosphatase; PPP_i, inorganic triphosphate; ThTP, thiamine triphosphate; ThTPase, thiamine triphosphatase; TTM, triphosphate tunnel metalloenzyme.

KEYWORDS

CYTH domain, inorganic triphosphate, tripolyphosphate, *Nitrosomonas*, polyphosphates, triphosphate tunnel metalloenzymes, thiamine triphosphatase, Mg²⁺, ATP.

LEGENDS TO FIGURES

FIGURE 1. **Structure of *NeuTTM*.** (A) Amino acid sequence and secondary structure elements. The residues conserved among known CYTH proteins (9) are highlighted by red boxes. (B) Cartoon representation of the *NeuTTM* monomer. Side chains of residues probably involved in substrate and divalent cation binding and/or catalysis are rendered as sticks and are labeled. (C) Stabilization of the open β -barrel structure by hydrophobic interactions with α -turn4 and α -helix5. The *NeuTTM* monomer is shown in a cartoon representation (grey). The residues forming a hydrophobic patch that stabilizes the protein core are shown in magenta sticks and labeled.

FIGURE 2. **Substrate specificity of recombinant His-tagged non-mutated *NeuTTM*.** The specificity was tested in the presence of (A) 5 mM MgCl_2 (pH 9.7) or (B) 1 mM MnCl_2 (pH 10.4). The incubation medium contained either 50 mM Na-CHES (pH 9.7) or 50 mM Na-CAPS (pH 10.4), 0.5 mM substrate, 5 mM MgCl_2 (pH 9.7) or 1 mM MnCl_2 (pH 10.4). The temperature was 37 °C. (Mean \pm SD, n = 2 - 6)

FIGURE 3. **Kinetic properties of *NeuTTM* PPPase activity.** The PPP_i concentration was 0.5 mM. (A) Dependence on temperature in the presence of 5 mM Mg^{2+} at pH 9.7 (\circ) or 0.8 mM Mn^{2+} at pH 10.4 (\bullet). (B) pH dependence in the presence of 10 mM Mg^{2+} (\circ) or 1 mM Mn^{2+} (\bullet) at 37 °C. (C) Dependence on substrate concentration at pH 7.1 (\circ) and 9.7 (\bullet) at 37 °C. The curves were drawn by non-linear regression of the Michaelis-Menten equation (n = 3). The buffers used for different pH values are given in the “Materials and Methods” section. (Mean \pm SD)

FIGURE 4. **Activation of *NeuTTM* PPPase by divalent cations.** (A) Dependence of PPPase activity on Mg^{2+} (\circ) and Mn^{2+} (\bullet) total concentration. The incubation was carried out in the presence of 50 mM Na-CHES (Mg^{2+} , pH 9.7) or Na-CAPS (Mn^{2+} , pH 10.4) at 37 °C. (B) Effect of increasing concentrations of Co^{2+} (calculated free Co^{2+} concentration assuming $K_d = 8$ nM for the Co-PPP_i complex) on the PPPase activity. Conditions of experiment: PPP_i , 0.5 mM; Na-CHES, 50 mM, pH 9.5, 45 °C. (Mean \pm SD, n = 3)

FIGURE 5. **Inhibition of *NeuTTM* PPPase by divalent cations.** (A) Inhibition by Ca^{2+} and Mn^{2+} in the presence of Mg^{2+} . The incubation medium contained: PPP_i , 0.5 mM, MgCl_2 5 mM, Na-CHES, 50 mM, pH 9.7 at 37 °C. (B) Effect of increasing concentrations of Mg^{2+} (calculated free $[\text{Mg}^{2+}]$) on *NeuTTM* PPPase activity in the presence or absence of Ca^{2+} ions at 50 °C. The incubation medium contained: PPP_i , 0.5 mM; Na-CHES, 50 mM, pH 9.7. (C) Effect of increasing concentrations of ZnSO_4 on the PPPase activity of *NeuTTM*. The incubation medium contained: PPP_i , 0.5 mM; MgCl_2 , 5 mM; Na-CHES, 50 mM, pH 9.7 at 37 °C. (Mean \pm SD, n = 3)

FIGURE 6. Mass spectra of His-tagged *NeuTTM* in the absence of added substrates and divalent cations. M = monomer (theoretical mass = 19,987.4 Da) and M₂ = dimer (theoretical mass = 39,974.8 Da). (A) Spectrum recorded in harsher source conditions (RF lens 1 voltage = 150 V): the dimer is partially destroyed but the mass accuracy is higher. (B) Spectrum recorded in soft source conditions (RF lens 1 voltage = 50 V), showing that the dimer is the most abundant species in solution. The protein concentration was 10 μM in 100 mM ammonium acetate (pH 6.5).

FIGURE 7. Mass spectra showing high specificity of *NeuTTM* for PPP_i compared to ATP and ThTP. (A) Spectrum of 10 μM protein alone in 100 mM NH₄OAc, pH = 6.5. (B) Same as (A) with 25 μM PPP_i. (C) Same as (A) with 20 μM protein and 50 μM ATP. (D) Same as (A) with 25 μM ThTP instead of PPP_i.

FIGURE 8. Detailed identification of complexes of *NeuTTM* (10 μM) in binary and ternary mixtures with MgCl₂ (0.1 mM) and/or PPP_i (25 μM). The spectra were all recorded in 100 mM ammonium acetate (pH 6.5) at an RF lens 1 voltage = 150 V for a more accurate mass determination of each complex. (A) *NeuTTM* alone at charge state 8+. The main peak corresponds to the uptake of eight protons and few sodium or potassium adducts are detected. (B) *NeuTTM* binary mixture with Mg²⁺. The intensity of unresolved adducts peaks increases, but the fully protonated protein remains the most intense peak. (C) *NeuTTM* binary mixture with PPP_i. The fully protonated complex is minor, and the major complexes take up two monovalent cations. (D) *NeuTTM* ternary mixture with PPP_i and Mg²⁺. The enzyme-substrate complex with the uptake of one Mg²⁺ is clearly detected.

FIGURE 9. pH-dependence of non-mutated *NeuTTM* and of the Y28F and K52R mutants. The reaction was carried out in the presence of 5 mM Mg²⁺ at 37 °C. The control values obtained in the absence of enzyme were subtracted. (A) V_{\max}/K_m as a function of pH for the non-mutated enzyme. (B) pH-dependence of V_{\max} of non-mutated (●) and K52R-mutated (▲) *NeuTTM*. (C) The activities of Y28F (○) and K52R (▲) mutants are expressed as percentage of the respective value obtained at pH 9.7 (100%). The PPP_i concentration was 0.1 mM. (D) pH-dependence of Y29F-mutated *NeuTTM*, [PPP_i] = 0.1 mM). (Mean ± SD, n=3-6)

FIGURE 10. **Proposed catalytic mechanism for PPP_i hydrolysis by *NeuTTM*.** The K52-Y28 pair is considered to form a catalytic dyad. The most simple and plausible mechanism is a general acid - general base catalysis with no covalent acyl-enzyme intermediate.

TABLE 1

X-ray data collection and refinement statistics. Statistics for the highest resolution bin are in parentheses.

Data collection	
Space group	P 3 ₂ 2 1
Unit cell (Å, °)	a= 52.28, b= 52.28, c = 252.48 α = β = 90.0 γ = 120.0
Wavelength (Å)	0.97959
Temperature (K)	100
Resolution (Å)	42.6-1.9 (1.95-1.9)
Observed reflections	32810 (2358)
$R_{\text{int}}^{\text{a}}$	0.057 (0.560)
Average redundancy	6.7 (4.9)
$\langle I \rangle / \langle \sigma(I) \rangle$	20.5 (2.3)
Completeness, %	99.7 (99.0)
Refinement	
R/R_{free}	0.213 (0.304) / 0.270 (0.358)
Protein atoms	2424
Water molecules	324
Other atoms	20
RMSD from ideal bond length (Å) ^b	0.02
RMSD from ideal bond angles [#]	2.1°
Average B-factor for protein atoms (Å ²)	30.3
Average B-factor for water molecules (Å ²)	39.8
Ramachandran plot statistics (%) ^c	
Allowed	100
Favored	98.3
Outliers	0

^a $R_{\text{int}} = \sum |I - \langle I \rangle| / \sum I$ where I is the intensity of an individual reflection and $\langle I \rangle$ is the mean intensity of a group of equivalents and the sums are calculated over all reflections with more than one equivalent measured

^b (23)

^c (22)

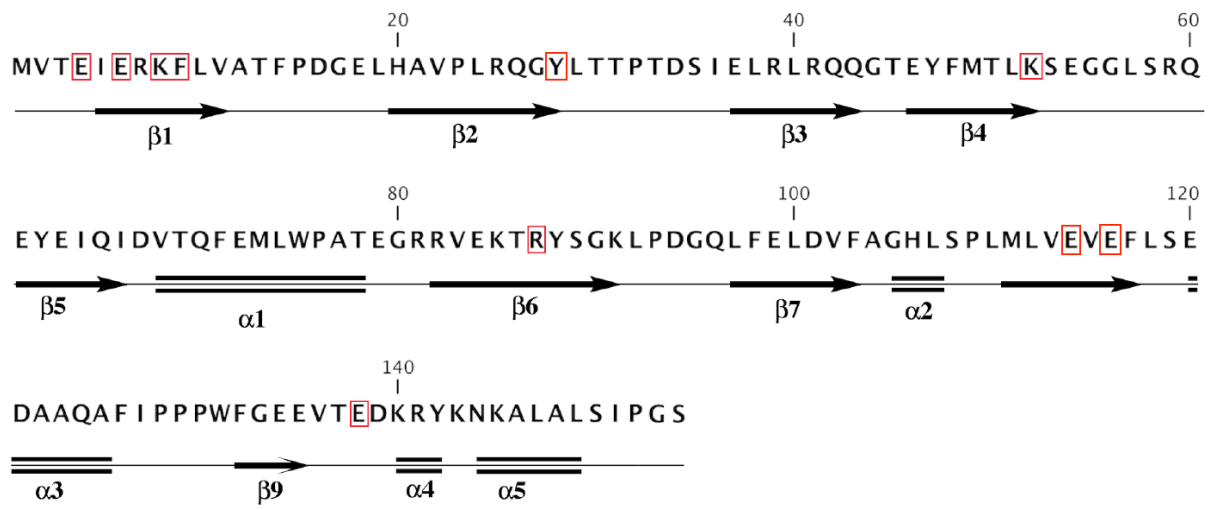
TABLE 2

Kinetic parameters for non-mutated (WT) and mutated recombinant *NeuTTM*. (Mean \pm SD, n = 3-4)

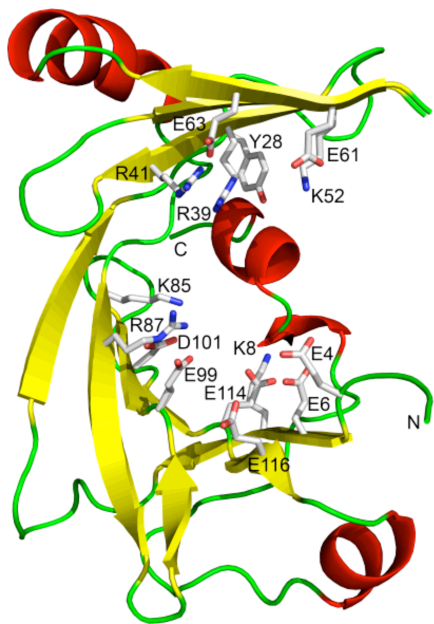
Enzyme preparation	Substrate	Conditions of experiment	$K_{m,app}$ μM	V_{max} $\mu mol\ min^{-1}\ mg^{-1}$	k_{cat} s^{-1}	k_{cat}/K_m s^{-1}/M^{-1}
WT His-tagged	PPP _i	50 °C, pH 9.7 [Mg ²⁺] = 5 mM	40 \pm 15	910 \pm 70	288	7.2 10 ⁶
		37 °C, pH 9.7 [Mg ²⁺] = 5 mM	21 \pm 3	240 \pm 30	76	3.6 10 ⁶
	ATP	37 °C, pH 7.1 [Mg ²⁺] = 5 mM	58 \pm 5	60 \pm 2	19	0.33 10 ⁶
		50 °C, pH 8.1 [Mn ²⁺] = 10 mM	800 \pm 120	1.2 \pm 0.2	0.36	0.45 10 ³
WT untagged	PPP _i	50 °C, pH 9.7 [Mg ²⁺] = 5 mM	100 \pm 20	25,000 \pm 2000	7900	79 10 ⁶
K8A His-tagged	PPP _i	50 °C, pH 9.7 [Mg ²⁺] = 5 mM	390 \pm 30	2800 \pm 500	887	2.3 10 ⁶
		37 °C, pH 9.7 [Mg ²⁺] = 5 mM	280 \pm 55	235 \pm 30	74	0.19 10 ⁶
	ATP	50 °C, pH 10.1 [Mn ²⁺] = 10 mM	1200 \pm 500	12.5 \pm 3.2	3.96	3.3 10 ³
K85A His-tagged	PPP _i	50 °C, pH 9.7 [Mg ²⁺] = 5 mM	720 \pm 60	65 \pm 7	21	29 10 ³
		37 °C, pH 9.7 [Mg ²⁺] = 5 mM	2600 \pm 400	33 \pm 3	10	4 10 ³
K52R His-tagged	PPP _i	37 °C, pH 9.7 [Mg ²⁺] = 5 mM	191 \pm 8	3.1 \pm 0.1	0.98	5.1 10 ³

FIGURE 1. Structure of *NeuTTM*.

A



B



C

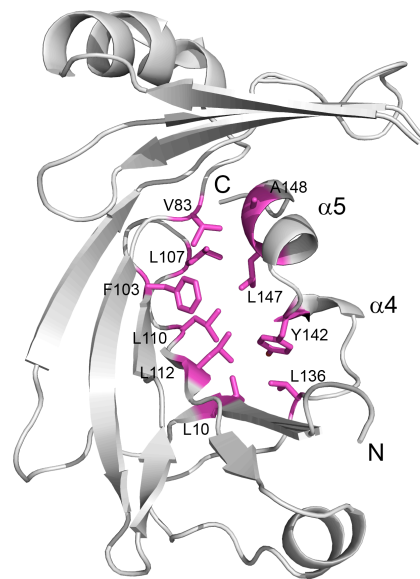


FIGURE 2. Substrate specificity of recombinant His-tagged non-mutated *NeuTTM*.

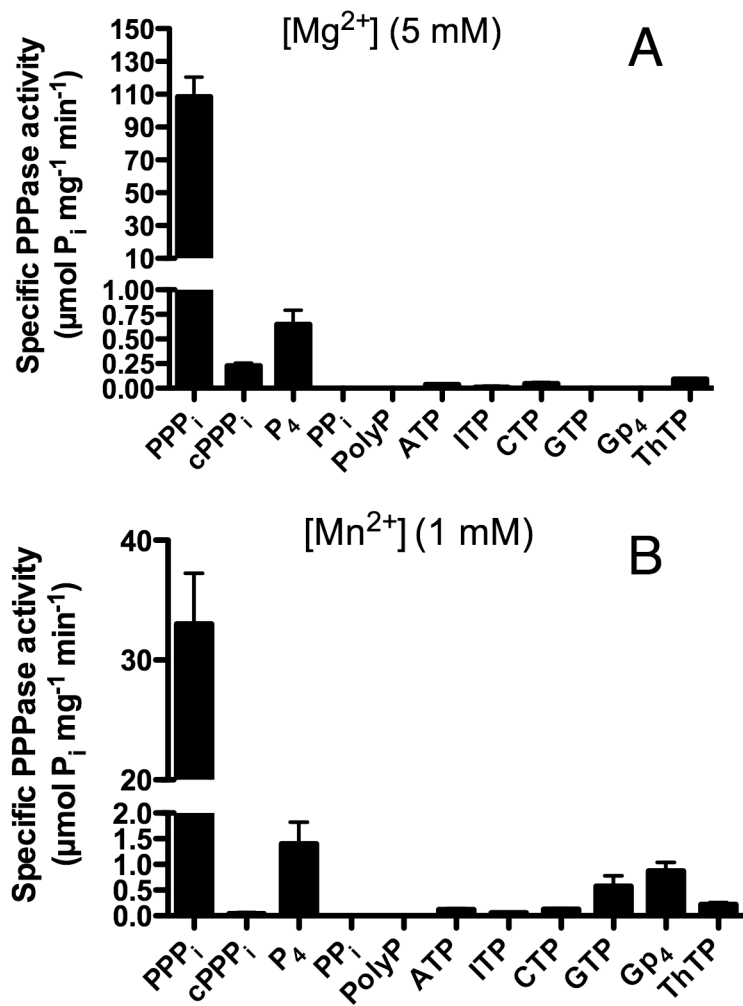


FIGURE 3. Kinetic properties of *NeuTTM* PPPase activity.

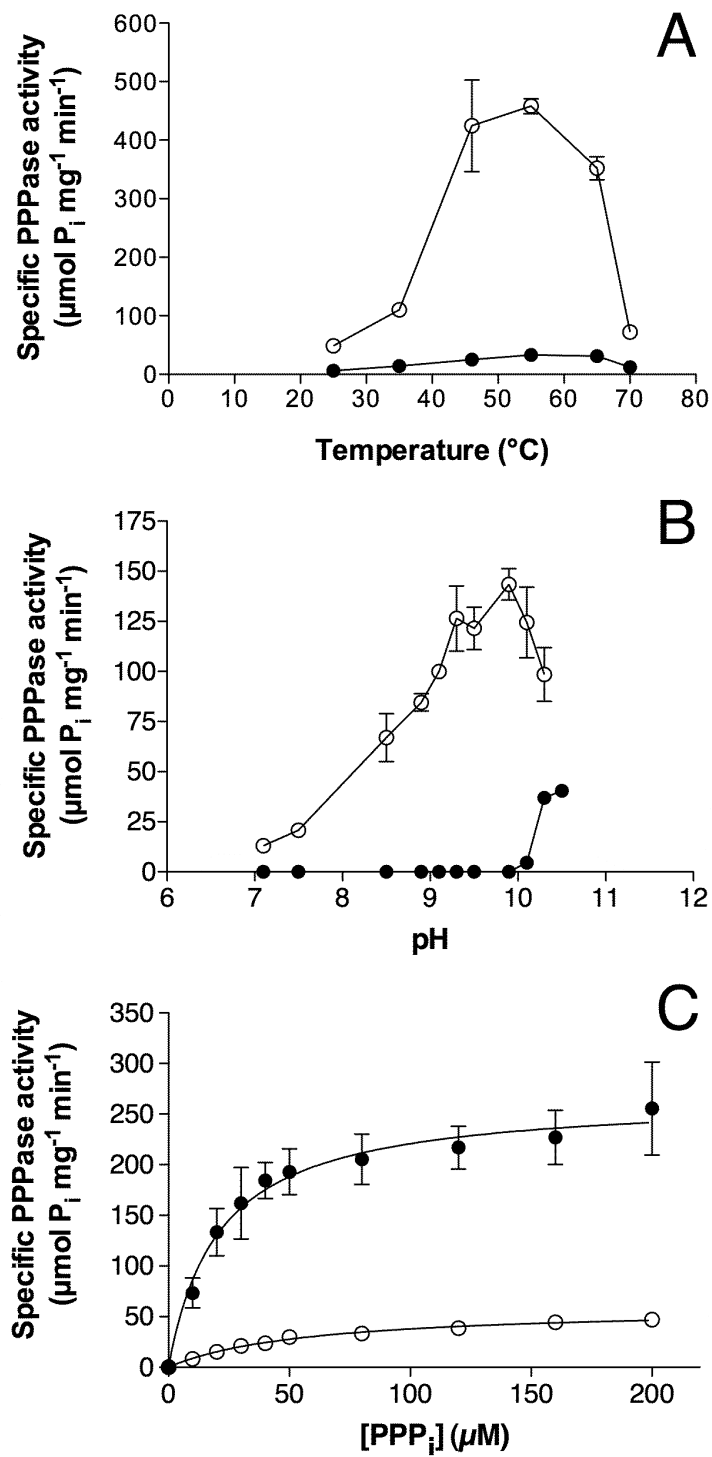


FIGURE 4. Activation of *Neu*TTM PPPase by divalent cations.

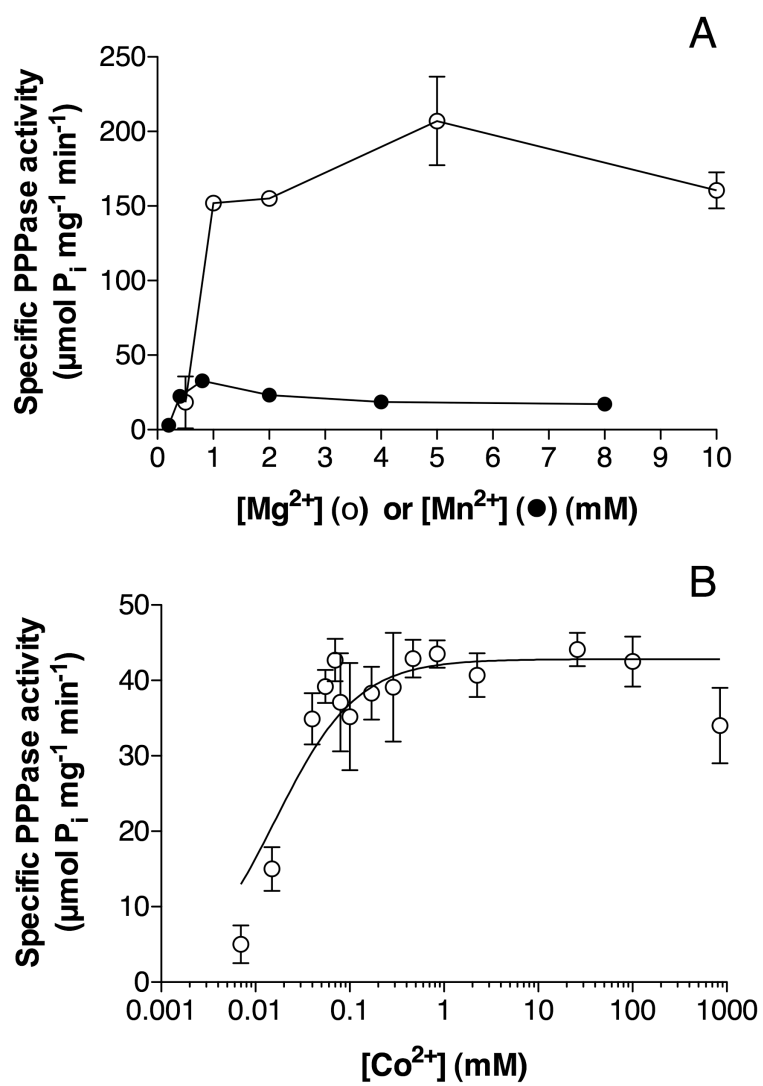


FIGURE 5. Inhibition of *Neu*TTM PPPase by divalent cations.

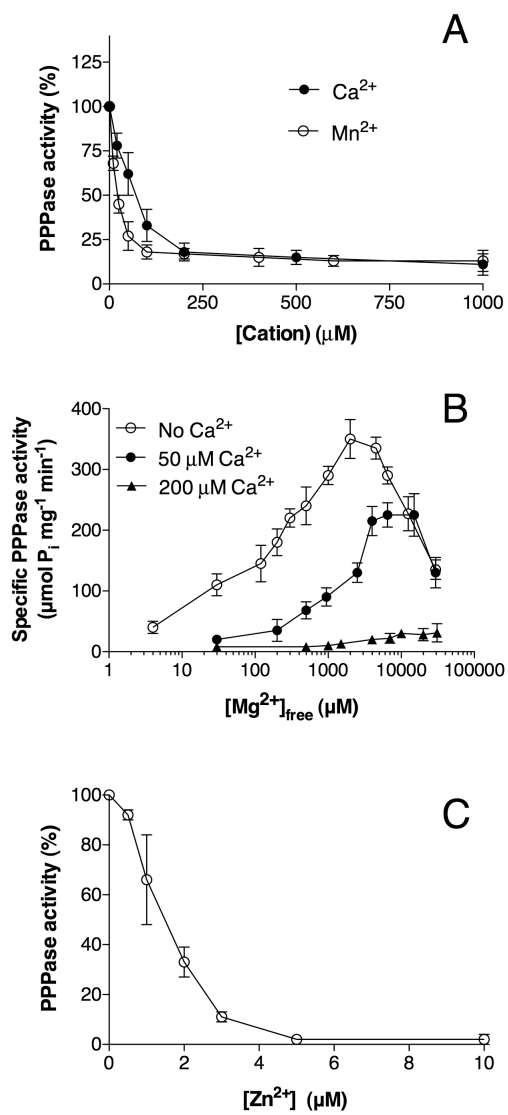


FIGURE 6. Mass spectra of His-tagged *NeuTTM* in the absence of added substrates and divalent cations.

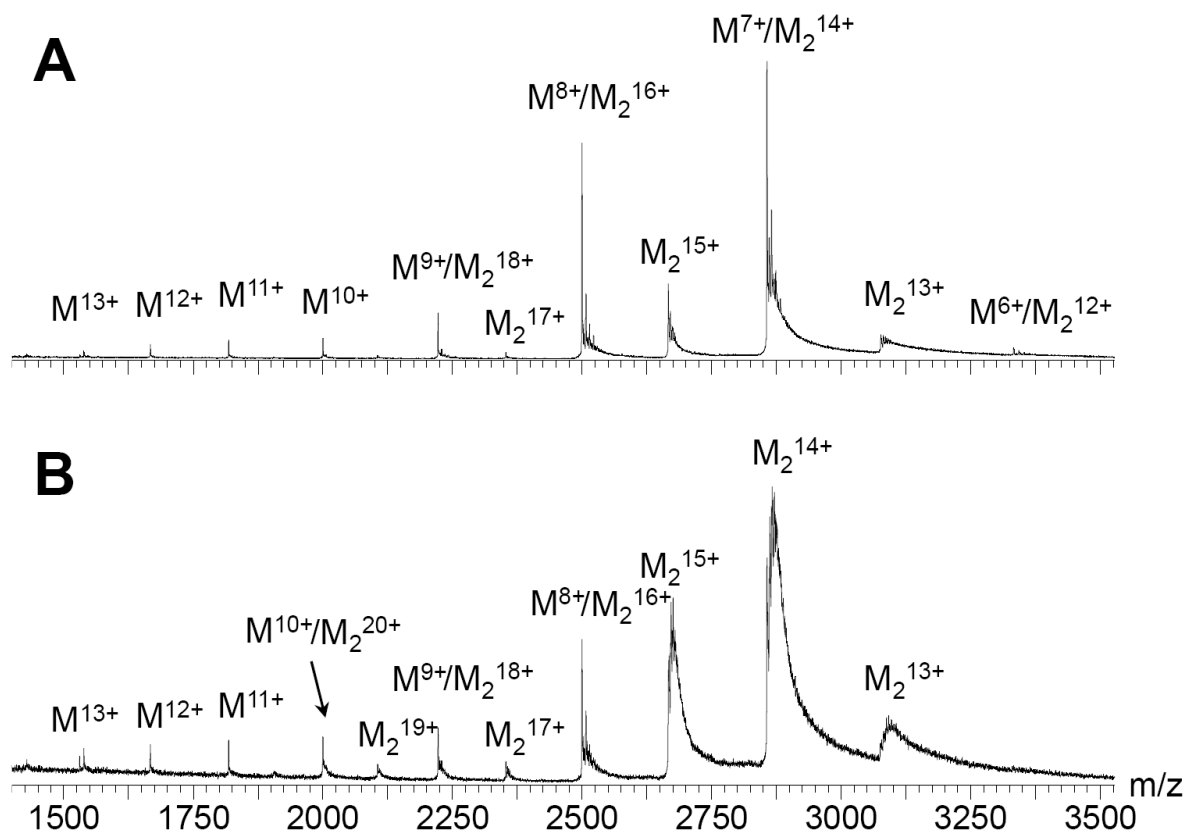


FIGURE 7. Mass spectra showing high specificity of *NeuTTM* for PPP_i compared to ATP and ThTP.

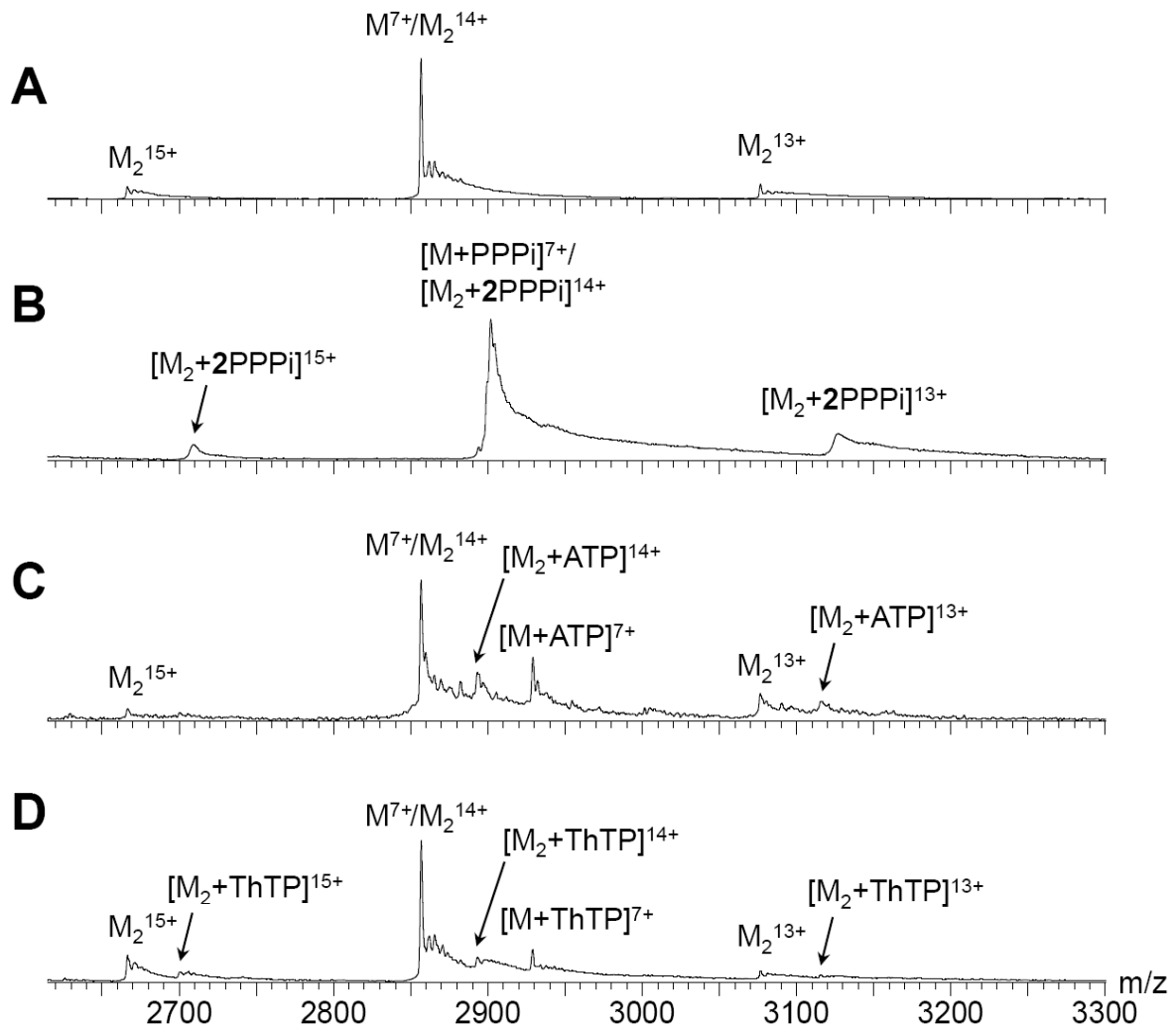


FIGURE 8. Detailed identification of complexes of *NeuTTM* (10 μM) in binary and ternary mixtures with MgCl_2 (0.1 mM) and/or PPP_i (25 μM).

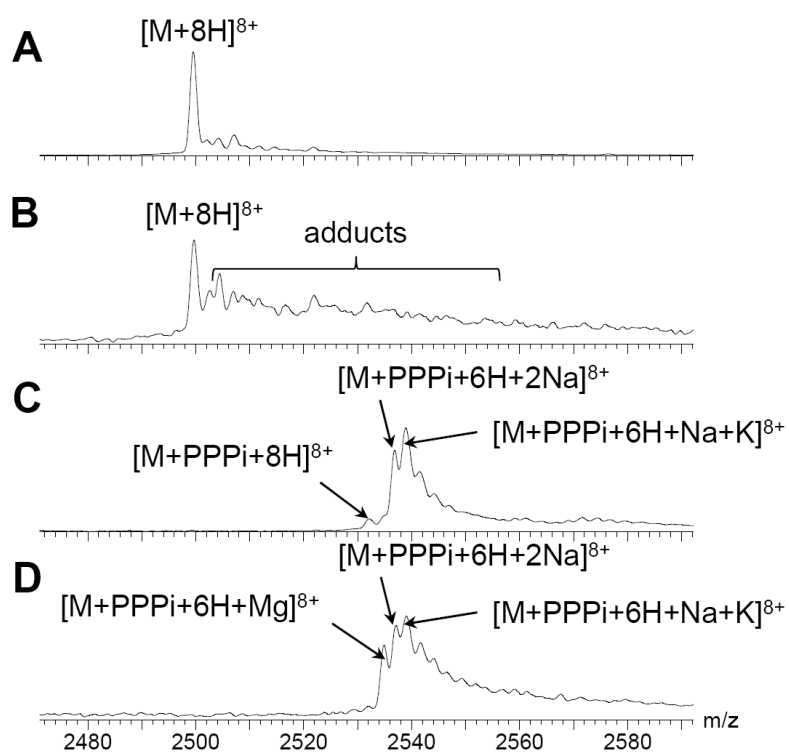


FIGURE 9. pH-dependence of non-mutated NeuTTM and of the Y28F and K52R mutants.

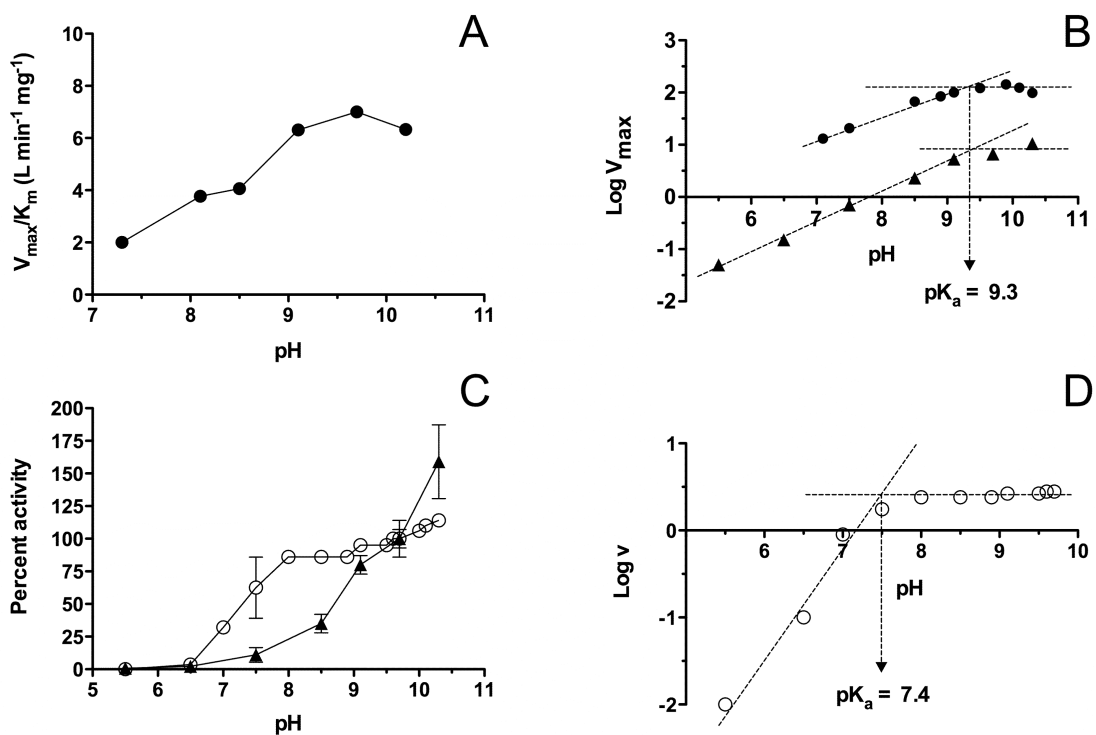
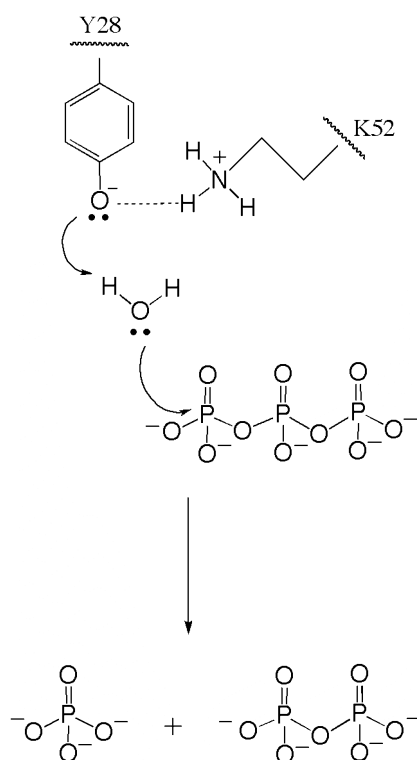


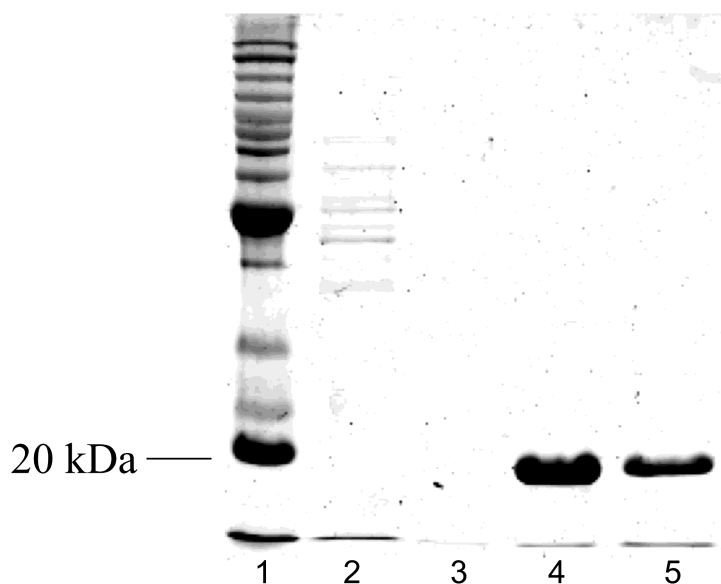
FIGURE 10. Proposed catalytic mechanism for PPP_i hydrolysis by *NeuTTM*.



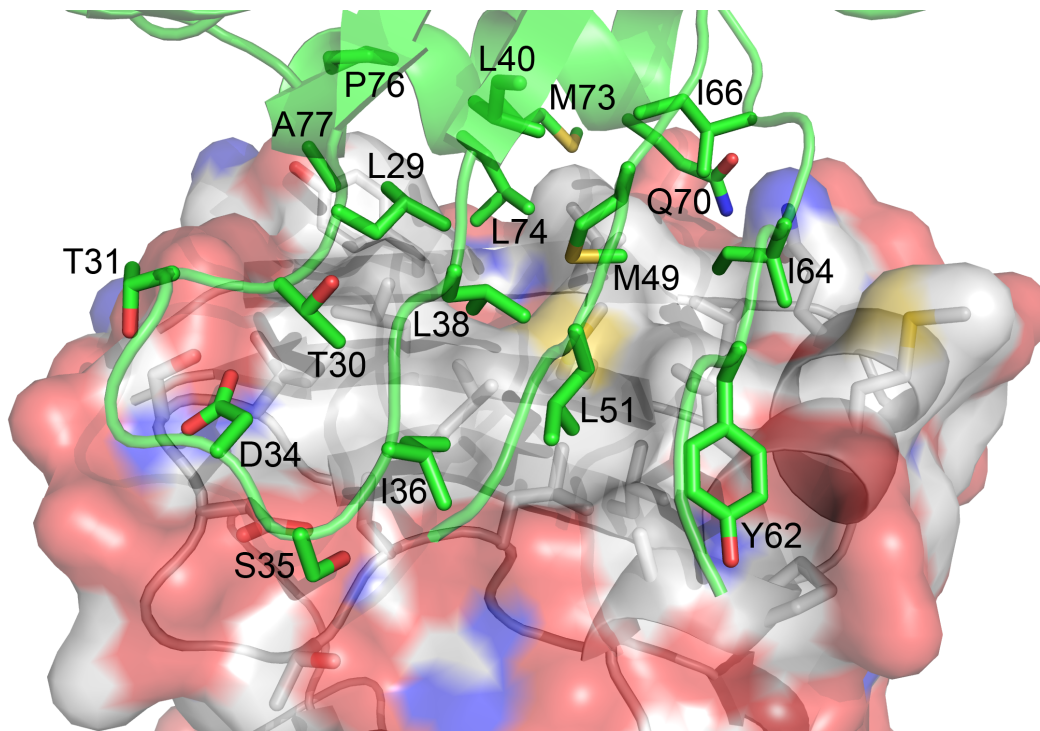
**A SPECIFIC INORGANIC TRIPHOSPHATASE FROM *NITROSOMONAS EUROPAEA*:
STRUCTURE AND CATALYTIC MECHANISM**

David Delvaux, Mamidanna R.V.S. Murty, Valérie Gabelica, Bernard Lakaye, Vladimir V. Lunin, Tatiana Skarina, Olena Onopriyenko, Gregory Kohn, Pierre Wins, Edwin De Pauw and Lucien Bettendorff

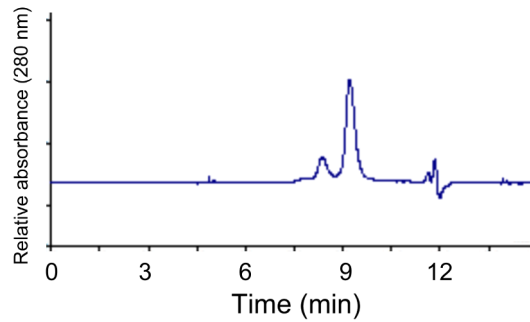
Supplemental data



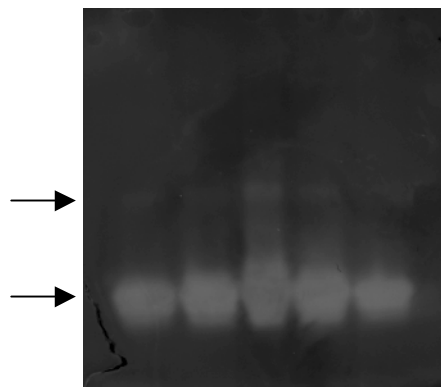
SUPPLEMENTAL FIGURE S1. SDS-PAGE after the different purification steps of polyHis-tagged *NeuTTM*. Lane 1, BenchMark™ Protein Ladder. Lane 2 and 3 represent the protein content of flow-through fractions that were eluted in binding buffer. Lane 4 and 5 represent the elution of His-tagged *NeuTTM* in elution buffer. It appears that almost all the protein of interest was recovered in the elution fractions and that the protein is very pure. The purification patterns of K8A, K85A, K52R and Y29F mutants were similar (not shown).



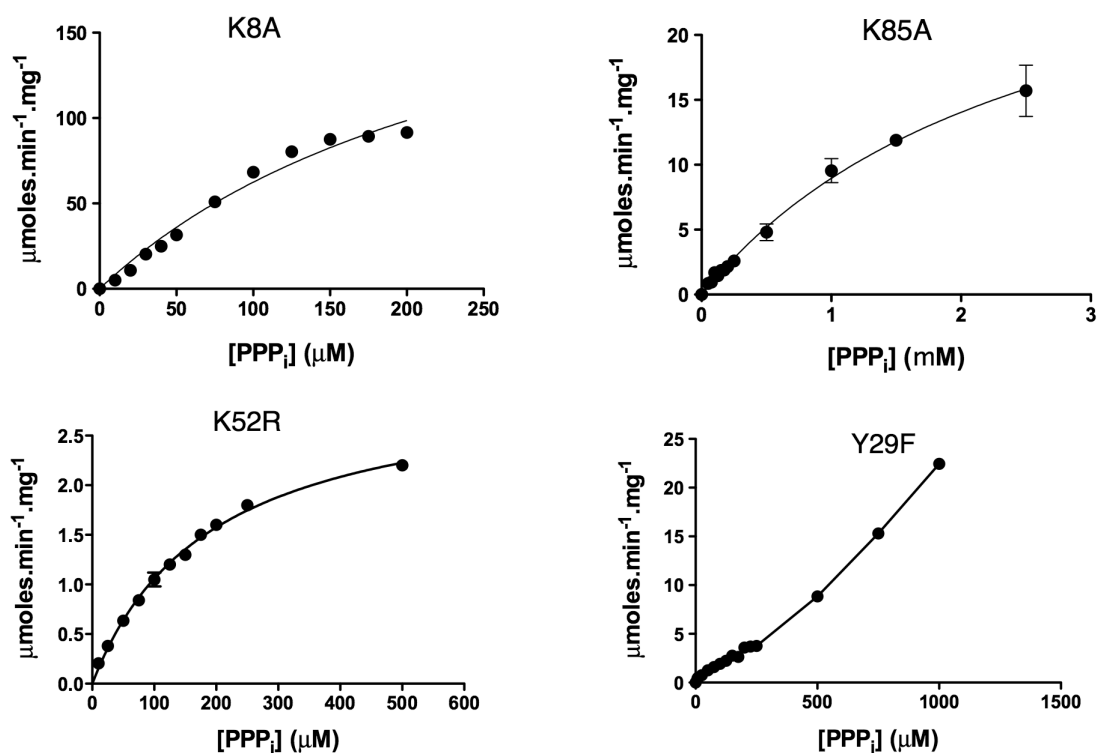
SUPPLEMENTAL FIGURE S2. **Dimerization interface of *NeuTTM***. Monomer A is shown in cartoon representation (green ribbon, green carbon atoms), while a semitransparent molecular surface is also rendered for the monomer B (grey carbon atoms). For both monomers, oxygen atoms are colored red, nitrogen atoms blue and sulfur atoms yellow. The residues forming the dimerization interface are shown as sticks for both monomers and labeled for monomer A.



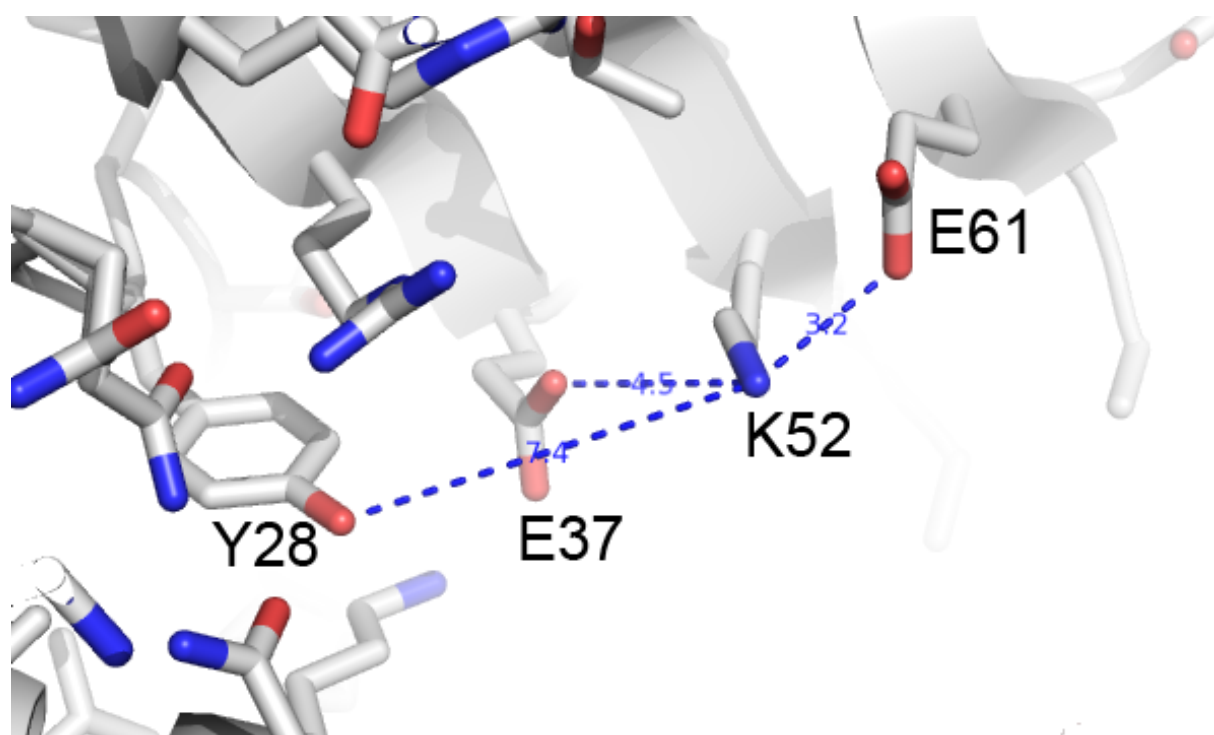
SUPPLEMENTAL FIGURE S3. **Separation of the monomer and the dimer of *NeuTTM* by size exclusion chromatography.** The TSK column (G3000SW, 30 x 0.75 cm, 7 mm) was equilibrated with 20 mM Hepes-Na (pH 6.8) and 200 mM NaCl at a flow rate of 0.5 ml/min. A volume of 20 μ l of the protein solution (1.75 mg of protein / ml) were injected and the two peaks were collected for determination of enzyme activities.



SUPPLEMENTAL FIGURE S4. **In-gel activity determination of *NeuTTM* PPPase activity.** The active bands are colored in white. The higher dot shows the band corresponding to the dimer and the lower one to the monomer.



SUPPLEMENTAL FIGURE S5. **Substrate concentration-dependence of the PPPase activity in four *NeuTTM* mutants.** The enzymes were incubated at 37 °C in the presence of 5 mM Mg²⁺ and 50 mM Na-CHES buffer, pH 9.7. The curves were obtained by non-linear regression of the Michaelis-Menten equation (n = 3) except for Y29A where a connecting line was used (n=6).



SUPPLEMENTAL FIGURE S6. The suggested catalytic dyad K52 and Y28 and the distances from K52NZ to the closest neighboring residues in the crystal structure.

SUPPLEMENTAL TABLE S1

Oligonucleotides used for site-directed mutagenesis. The modified bases are in bold and underlined.

Primer	Sequence
K8A	Forward : 5'-CCGAGATCGAACG <u>C</u> CATTTCTCGTGGCAACTT-3' Reverse : 5'-AAGTTGCCACGAGAAAT <u>G</u> CGCGTTCGATCTCGG-3'
K85A	Forward : 5'-GCGGCGTGTAGAG <u>G</u> CAACCCGGTACAGTG-3' Reverse : 5'-CACTGTACCGGGTT <u>G</u> CCTCTACACGCCGC-3'
Y28F	Forward : 5'- CCGCTCCGTCAGGGCT <u>T</u> TCTGACCACCCACAG-3' Reverse : 5'- CTGTGGGGGTGGTCAGAA <u>A</u> AGCCCTGACGGAGCGG-3'
K52R	Forward : 5'- GAATATTTTCATGACGCTG <u>A</u> GATCCGAGGGTGGATTA-3' Reverse : 5'- TAATCCACCCTCGGAT <u>C</u> TCAGCGTCATGAAATATTC-3'

SUPPLEMENTAL TABLE S2

PPPase activity of His-tagged K85A mutant *NeuTTM* in the presence of various concentrations of PPP_i and divalent cations. Incubations were carried out at 50 °C, pH 9.7 (n = 3-4).

[PPP _i]	Divalent cation	Divalent cation (free concentration)	Specific activity
<i>mM</i>		<i>mM</i>	$\mu\text{mol}\cdot\text{min}^{-1}\cdot\text{mg}^{-1}$
0.5	Mg ²⁺	2	4.0 ± 0.3
	Mg ²⁺	5	4.2 ± 0.3
	Mn ²⁺	1	6.0 ± 2.5
	Mn ²⁺	4	18 ± 4
	Co ²⁺	2	0.8 ± 0.6
	Zn ²⁺	1	2.0 ± 0.5
	Zn ²⁺	4	10 ± 2
2	Mg ²⁺	2	27 ± 6
	Mg ²⁺	5	55 ± 4
	Mn ²⁺	1	80 ± 9
	Mn ²⁺	4	70 ± 6
	Co ²⁺	2	18 ± 6
	Zn ²⁺	1	22 ± 7
	Zn ²⁺	4	27 ± 5